https://doi.org/10.5194/cp-2023-101
Preprint. Discussion started: 4 January 2024

Climate of the Past
Discussions

Title: *Nordic Seas Deep-Water susceptible to enhanced freshwater export to the subpolar North Atlantic during peak MIS 11*

Michelle J. Curran [a], Christophe Colin [b], Megan Murphy O'Connor [a,c], Ulysses Ninnemann [d], and Audrey Morley [a,c,*]

[a] *School of Geography, Archaeology and Irish Studies, and The Ryan Institute at the University of Galway, H91TK33 Galway, Ireland.*
[b] *Université Paris-Saclay, CNRS, GEOPS, 91405, Orsay, France*
[c] *iCRAG – Irish Centre for Research in Applied Geosciences, Belfield, Dublin 4, Ireland*
[d] *Department of Earth Science and Bjerknes Centre for Climate Research, University of Bergen, Bergen, Norway*

** Corresponding Author*

Abstract

Recent investigations into Marine Isotope Stage (MIS) 11 (424-403 ka), an unusually long and warm interglacial of the Quaternary Period, have found that the Atlantic Meridional Overturning Circulation remained strong while background melting of the Greenland Ice-Sheet (GIS) was high, and resulted in a fresh and cold surface ocean in the Nordic Seas. These investigations support the hypothesis that deep-water formation may not be as susceptible to future GIS melting as previously thought. Here we test this hypothesis and present a palaeoceanographic investigation of a freshwater-related abrupt climate event recorded in the eastern North Atlantic during peak interglacial conditions (~412 ka), when the GIS was as small or smaller than today. Using sediment core DSDP-610B recovered from the western Rockall Trough we reconstruct the evolution of Nordic Seas Deep-Water (NSDW) using benthic carbon isotope, Neodymium isotopes, and grain-size analysis paired with end-member modelling. Further, a combination of planktonic foraminiferal assemblage census and Ice-Rafted Debris counts allow us to reconstruct surface water properties including temperature and the movement of oceanic fronts throughout this event. Our results demonstrate that a reduction of NSDW only occurs once GIS melt and polar freshwater reaches subpolar latitudes. We hypothesise that the reorganisation of fresh and cold surface waters from the Nordic Seas into the subpolar North Atlantic was responsible for an AMOC-related cold event centred at 412 ka. Placing our results in the palaeogeographical context of the North Atlantic Region we tentatively propose that the ocean-atmosphere climate dynamics linking the Nordic Seas with the subpolar North Atlantic played and will play a crucial role for the stability of NSDW formation in the future, considering the enhanced melting and overall hydrological cycle at high Northern latitudes predicted for future climate scenarios.

1 Introduction

https://doi.org/10.5194/cp-2023-101
Preprint. Discussion started: 4 January 2024

Modern Greenland Ice-Sheet (GIS) melting is a response to increased global mean temperatures driven by rising greenhouse gas emissions (Aguiar et al., 2021;Fettweis et al., 2017;Tedesco and Fettweis, 2012;Golledge et al., 2019). The addition of meltwater has the potential to alter surface water buoyancy (Østerhus et al., 2001;Praetorius et al., 2008) and thereby deep-water formation (Galaasen et al., 2014;Bond et al., 1997) at high-latitudes. This is pertinent for future climate change scenarios, as multiple modelling studies suggest that the strength of the Atlantic Meridional Overturning Circulation (AMOC) may be impacted by meltwater (Stommel, 1961;Rahmstorf, 1995;Caesar et al., 2018), derived from the GIS (Bakker et al., 2016;Böning et al., 2016;Luo et al., 2016;Yu et al., 2016). Modern observations over the past 30 years, however, do not confirm a decline or sustained weakening of the AMOC in response to increased freshwater export to deepwater formation regions (Worthington et al., 2021), highlighting the need for longer observations reaching beyond instrumental datasets.

Past archives of North Atlantic Deep Water (NADW) variability provide us with a tool to assess NADW stability and response to changing climate boundary conditions. This is important as recent palaeo studies by Caesar et al. (2021) and Thornalley et al. (2018) suggest the AMOC is currently at its weakest state for the past ~150 years. Thornalley et al. (2018) link the AMOC slowdown to freshwater runoff from the GIS. Therefore, it is crucial to improve our understanding of how surface and deep-water components within the North Atlantic are linked, and on what time frames they respond to freshwater-induced climate instabilities during interglacial climate boundary conditions. Past interglacials provide a good analogue to enhance our understanding of the complex nature of the climate system (Yin and Berger, 2015). In particular, periods with sufficiently similar boundary conditions to the present day can meaningfully advance our understanding of the antecedents and mechanisms generating variability and instability in the climate system.

Marine Isotope Stage (MIS) 11 began at ~424 ka (Lisiecki and Raymo, 2005) and was a particularly long, ~30 ka, interglacial (Howard, 1997;McManus et al., 1999;Reyes et al., 2014), covering two precessional cycles (Laskar et al., 2004). Unlike the current Holocene, the manifestation of the climate optimum occurred relatively late into the interglacial, i.e., after ~410 ka (Ruddiman, 2005;Tzedakis et al., 2012;McManus et al., 1999;Kandiano and Bauch, 2007;Dickson et al., 2009), most likely due to the anti-phasing of precession and obliquity (Laskar et al., 2004). Nevertheless, MIS 11 is often cited as a good analogue for our current interglacial (Tzedakis et al., 2012;Droxler et al., 2003;Berger and Loutre, 2002;Loutre and Berger, 2003;Candy et al., 2014;Tzedakis, 2010;Mcmanus et al., 2003) due to persistently high atmospheric CO_2 concentrations (Petit et al., 1999;Raynaud et al., 2005;Nehrbass-

https://doi.org/10.5194/cp-2023-101
Preprint. Discussion started: 4 January 2024

Climate of the Past
Discussions

Ahles et al., 2020), similar to preindustrial Holocene values (Bazin et al., 2013) (Figure 1), and dampened precession modulated by an eccentricity minimum (Berger and Loutre, 1991;Bauch et al., 2000;Hodell et al., 2000;Dickson et al., 2009;Loutre and Berger, 2000;Bazin et al., 2013).

The peaks in precession at 424 ka and 408 ka (Pol et al., 2011;Tzedakis, 2010), contributed to protracted high-latitude warming. Paired with high CO_2 concentrations these boundary conditions resulted in excessive GIS melt/retreat culminating in minimum GIS extent at ~403 ka (Robinson et al., 2017a). Due to the retreat of high-latitude ice sheets, MIS 11 had relative sea levels ~6 to 13 metres above present-day values, peaking at ~403 ka (PAGES, 2016;Reyes et al., 2014;Robinson et al., 2017a;Raymo and Mitrovica, 2012). Further, terrestrial archives provide evidence for sustained warming of the North Atlantic and Arctic regions during MIS 11 (Melles et al., 2012;Desprat et al., 2005a;Nitychoruk et al., 2005;Prokopenko et al., 2010;SHICHI et al., 2009;Ashton et al., 2008;Preece et al., 2007;Reille et al., 2000;Tzedakis et al., 1997;Tzedakis et al., 2006) demonstrating warmer than present boundary conditions at least at high Northern latitudes. However, several palaeoceanographic studies document lower than present Sea Surface Temperature (SST) in the Nordic Seas (Kandiano et al., 2016;Helmke and Bauch, 2003;Bauch et al., 2000;Doherty and Thibodeau, 2018;Thibodeau et al., 2017;Kandiano et al., 2012).

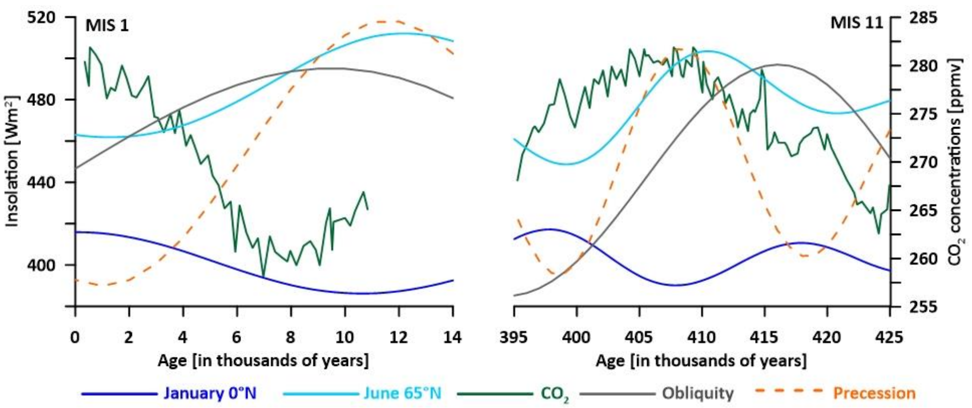

Figure 1: Climate forcings during MIS 1 and MIS 11. January insolation at 0°N [dark blue], June insolation at 65°N [light blue], Obliquity [grey], and Precession [dashed orange] (Laskar et al., 2004). Antarctica CO_2 (ppmv) [green] – MIS 1 (Bazin et al., 2013) – MIS 11 (Nehrbass-Ahles et al., 2020).

The leading hypothesis explaining these low SSTs postulates that the prolonged high-latitude warming enhanced freshwater export via melting from adjacent ice-sheets (Thibodeau et al., 2017;Kandiano et al., 2017a) and/or amplified Eurasian river runoff (Doherty and Thibodeau, 2018) throughout MIS 11 (de Vernal and Hillaire-Marcel, 2008;PAGES, 2016;Reyes et al., 2014). Increased freshwater at high latitudes then likely resulted in cool and relatively fresh buoyant surface water (Kandiano et al., 2017a;Thibodeau et al., 2017;Kandiano et al., 2012) at least until ~411 ka (Kandiano et al., 2012). Yet, despite the presence of freshwater, Nordic Sea Deep Water (NSDW) formation is believed to have been generally vigorous throughout MIS 11 (Dickson et al., 2009;Riveiros et al., 2013;McManus et al., 1999) although it's short-term stability/variability has been questioned (Galaasen et al. 2020). This scenario is contrary to models (Brodeau and Koenigk, 2016;Stouffer et al., 2006) and palaeo-observations of the recent past (Caesar et al., 2021;Thornalley et al., 2018).

An abrupt climate event at ~412 ka on past thresholds for reorganizing the climate-circulation regime as the boundary conditions (e.g. freshwater fluxes and distribution) evolve within the Nordic Seas and North Atlantic Basin. This event is recorded as a sea surface cold event (Kandiano et al., 2017b;Barker et al., 2015;Irvalı et al., 2020;McManus et al., 1999;Alonso-Garcia et al., 2011) across the subpolar North Atlantic. A concurrent perturbation of stable carbon isotopes (δ^{13}C) measured on benthic foraminifera (Galaasen et al., 2020;Hodell et al., 2008;McManus et al., 1999;Riveiros et al., 2013) further suggests a connection with the deep ocean. Continuous background melting or an abrupt meltwater discharge from the GIS, have been proposed as a trigger for this event, similar to events identified during other interglacials of the Quaternary (Galaasen et al., 2014;Galaasen et al., 2020;Irvalı et al., 2020;Irvalı et al., 2016). However, the mechanisms and phase relationships linking the release of freshwater across the Subpolar Gyre (SPG) to a slowdown in NSDW, remain elusive due to the low temporal resolution of existing records.

Here we present a detailed investigation of the climate-ocean perturbation at 412-ka, focusing on the temporal evolution (leads/lags) between surface and deep-water changes, within the eastern North Atlantic. We reconstruct both SST and deep-water properties from the same samples of Deep Sea Drilling Project (DSDP) site 94-610B (610B). Site 610B lies in the path of both the surface North Atlantic Current (NAC) and deep-water Wyville-Thomson Overflow Water (WTOW), a conduit of NSDW. This unique location and approach allow us to assess the relative timing between climate forcing and the response in the surface and deep branch of the AMOC located in the eastern North Atlantic. We are thus able to test the hypothesis linking background melting to a weakening of NSDW formation. Specifically, we aim to improve our mechanistic understanding of the climate response to meltwater forcing – a mechanism likely pertinent to the future evolution of the ocean-atmosphere climate system.

2 Hydrographic setting and materials

Modern sites for deep-water formation in the North Atlantic are the Nordic Seas and the subpolar North Atlantic, including the Irminger and Labrador Seas (Sgubin et al., 2017a). Overturning in the Nordic Seas is primarily modulated by thermohaline forcing (Hansen and Østerhus, 2000). The

https://doi.org/10.5194/cp-2023-101
Preprint. Discussion started: 4 January 2024

production of Iceland Scotland Overflow Waters (ISOW) and the Denmark Strait Overflow Waters (DSOW) creates density and pressure gradients at depths that drive overflow transport (Hansen and Østerhus, 2000;Olsen et al., 2008). As a result the outflow at depth creates a pressure gradient at the surface between the North Atlantic and the Nordic Seas (Jungclaus et al., 2006a;Mauritzen, 1996;Doherty et al., 2021;Olsen et al., 2008;Østerhus et al., 2001;Hansen and Østerhus, 2000) forcing a compensating inflow of Atlantic Waters into the Nordic Seas (Østerhus et al., 2001;Hansen and Østerhus, 2000). Thus, deep-water formation in the Nordic Seas (NSDW) may continue despite enhanced freshening, as long as a density gradient across the Greenland-Scotland Ridge, connecting the Atlantic and the Nordic Seas, is maintained (Østerhus et al., 2001) and the inflow of Atlantic Water via wind stress continues (Sandø et al., 2012). Overturning in the Irminger and Labrador Seas mainly occurs in winter as a result of buoyancy loss to the atmosphere (Sgubin et al., 2017a;Brodeau and Koenigk, 2016). As a result these sites likely respond more rapidly to freshwater input (Latif et al., 2006), which could stabilise the water column and thereby weaken overturning, as modelled by Jungclaus et al. (2006a) and Olsen et al. (2008). To assess the full impact of freshwater on the variability and strength of deep-water formation, long-term observations are required because of the decadal to multidecadal integration of surface water variability in the deep ocean (Buckley and Marshall, 2016). However, in-situ observations are only available since 2004 (Smeed et al., 2018) leaving us with a gap in our understanding of how NADW responds to sustained freshwater forcing.

Site 610B was recovered from the Feni Drift in the Rockall Trough, in the eastern North Atlantic at 53°13.297'N, 18°53.213'W; 2417 metres below sea-level (m) (Figure 2). The Feni Drift is a sedimentary contourite formed by overflow currents between the early Oligocene (33.9-23 Ma) and late Pliocene (3.6-2.58 Ma), with high accumulation rates on the crest of the Drift during the Pleistocene (Naylor and Shannon, 2005;Robinson and McCave, 1994;Flood et al., 1979). High-resolution (3.5 kHz) seismic profiles of the core site show tectonically stable sediment waves that have not migrated since the late Pliocene (Kidd and Hill, 1987, 1986); therefore we infer that the sedimentary sequence at the core site remained intact throughout the Quaternary.

At the surface the Rockall Trough directs ~50% of Atlantic Waters into the Nordic Seas (Hansen and Østerhus, 2000), thereby providing high-salinity Atlantic Waters for NSDW formation. There are two major sources of surface waters in the Rockall Trough: NAC derived from the Gulf of Mexico (Sutton and Allen, 1997) and subtropical gyre (STG) derived waters (Hátún et al., 2005). At depth, NSDW enters the Rockall Trough via Wyville-Thompson Ridge as Wyville-Thompson Overflow Water (WTOW) (Ellett et al., 1986;Johnson et al., 2017), and accounts for 10-15% of southward flowing NSDW (Dickson and Brown, 1994; Hansen and Østerhus, 2000). Unlike other water masses in the Rockall Trough, WTOW is the only water mass that enters from the north and flows south along the western margin of the Rockall Trough (Johnson et al., 2010). WTOW is limited to the western boundary of the Trough and is linked with the sedimentary contourite deposits of the Feni Drift (Holliday et al., 2000;Ellett and Martin, 1973). The southward flow of deep WTOW is intermittent on annual timescales but positive on decadal timescales (Johnson et al., 2017). To the north and west of site 610B the central anticyclonic gyre of the Rockall Trough (Johnson, 2012; New and Smythe-Wright, 2001; Smilenova et al., 2020), recirculates water down to 2000m during winter mixing (Smilenova et al., 2020). Given the distance from the gyre (ca 500 km) and the deeper depth of site 610B, it is unlikely that this influences the sedimentation and flow over the site. Modern hydrographic data thus indicates that site 610B lies in the pathway of poleward flowing Atlantic Waters at the surface and southward flowing WTOW at depth (Ellett et al., 1986;Johnson et al., 2017). The paired surface and deep-water reconstructions at site 610B are thus ideal to record both surface and deep-water flow variability in the eastern North Atlantic.

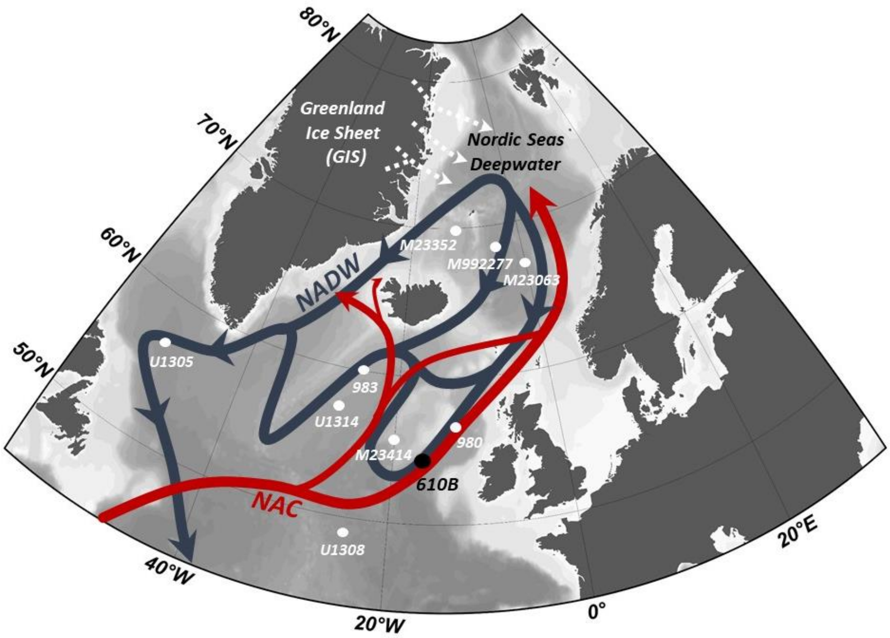

Figure 2: Schematic representation of the North Atlantic Ocean and Nordic Seas with arrows indicating the circulation components of the Atlantic Meridional Overturning Circulation (AMOC) in the North Atlantic basin. Major ocean currents include the North Atlantic Current (NAC) in red, deep-water originating in the Nordic Seas (NSDW) in blue, the Greenland Ice-Sheet (GIS), and freshwater influx routes to the Nordic Seas in white. Also shown in black are site 610B (this study), site M23414, M992277, M23352, M23063, Ocean Drilling Project (ODP) sites 980, and 983, and Integrated Ocean Drilling Program (IODP) sites U1314, U1305, and U1308 marked by white circles. The grey scale signifies bathymetry (GEBCO 2014), and was generated with Ocean Data View software (http://odv.awi.de/).

https://doi.org/10.5194/cp-2023-101
Preprint. Discussion started: 4 January 2024

3 Methods

Here we present data with a sampling resolution of 2.5 cm, between 28.6-29.7 metres below sea-floor (mbsf), and ~4 cm resolution between 29.74-29.83 mbsf, totalling 54 samples. Each sample was split and ~1 g of dry sediment was reserved for grain size analysis when samples had enough sediment available for analysis. The remaining sample was disaggregated on a Stuart SSL1 orbital shaker and washed at >63 μm. Following CLIMAP and Members (1976) selection of foraminiferal specimens for census and Ice-Rafted Debris (IRD) counts were performed after dry sieving to >150 μm.

3.1 Planktonic foraminiferal counts and species abundance (%)

Each sample was split using a micro-sample splitter into aliquots containing ~300 planktonic foraminiferal specimens. We identified, counted, and stored each specimen within a sample in identification slides. The absolute number of planktonic foraminifera counted ranged from 300-445. We use the abundance records (e.g., *Neogloboquadrina pachyderma*, (Np), *Turborotalita quinqueloba,* (*T. quinqueloba*)) to reconstruct the advance and retreat of the Polar and Sub-Arctic Fronts (Alonso-Garcia et al., 2011;Mokeddem et al., 2014). Here we define the Polar Front as the boundary between Polar and Arctic Waters, and the Sub-Arctic Front (SAF) as the boundary between Arctic and Atlantic Waters. In the modern ocean Np is the predominant foraminifera north of the Polar Front (Kipp, 1976) and is thus associated with Polar Waters from high-latitudes (Kohfeld et al., 1996;Pflaumann et al., 1996). *T. quinqueloba* is linked to the SAF (Loubere, 1981;Johannessen et al., 1994), with maximum abundance observed on the warmest side of the SAF (Johannessen et al., 1994). The Np coiling ratio is commonly used to infer changes in SST, e.g., Irvalı et al. (2016). We calculate the coiling ratio as Np/(Np + *N. incompta*)*100.

3.2 Sea Surface Temperature (SST) reconstruction

We used the ForCenS database (Siccha and Kucera, 2017) and the ROIJA package (Juggins, 2017) in R (Team, 2019), and a squared chord distance (dissimilarity measure), to estimate Modern Analogue Technique (MAT)-derived SSTs (Hutson, 1980;Prell, 1985). Here we chose to reconstruct annual SST from World Ocean Atlas 98, rather than seasonally based SST, because planktonic foraminifera inhabit a wide vertical range within the water column, and exhibit distinct variability in their seasonal abundance (Jonkers et al., 2013). This is particularly persuasive at subpolar latitudes and specifically during interglacial climates when many subpolar species display a double peak in abundance, one in spring and one in late summer (Chapman, 2010). Thus, annual reconstructions are likely more representative of assemblage ecological preferences. A high dissimilarity coefficient indicates poor

https://doi.org/10.5194/cp-2023-101
Preprint. Discussion started: 4 January 2024

modern analogues, with no similar analogue existing in the core-top database. Core tops with dissimilarity >0.4 were not considered. In this study the average SST standard deviation is 1.6°C.

3.3 Ice-Rafted Debris (IRD) counts

The relative abundance of IRD is an established proxy of ice sheet variability (Baumann et al., 1995; Fronval and Jansen, 1997; Jansen et al., 2000). All grains >150 µm in the aliquots split for census identification were counted. 10% of samples were recounted to determine the standard error. The average standard error for IRD counts in this study was 0.9%. We statistically compared the IRD counts using a t-test (two-sample t-test, $p < 0.05$) and found the differences to be insignificant (*d.f.*=4, t=2.78, p=0.2). We present the results as the number of lithogenic/terrigenous grains per gram (grains/g) of dry sediment.

3.4 Stable Isotope Analysis

Stable isotopes of oxygen and carbon were measured from the tests (<150 µm) of benthic foraminifera *Cibicidoides wuellerstorfi*. In total 60 samples were analysed between 28.55 – 29.955 mbsf. Stable isotope analyses were measured using a Kiel IV and MAT253 mass spectrometer at FARLAB at the Department of Earth Science and the Bjerknes Centre for Climate Research, University of Bergen. Results are expressed as the average of the replicates and reported relative to Vienna Pee Dee Belemnite (VPDB), calibrated using NBS-19 and crosschecked with NBS-18. Long-term reproducibility (1σ SD) of in-house standards for samples between 10 and 100 mg is better than 0.08‰ and 0.03‰ for $\delta^{18}O$ and $\delta^{13}C$, respectively.

3.5. *Neodymium isotope measurements on planktic foraminifer*

In total 17 samples of 15 to 30 mg of mixed planktonic foraminifera of size fraction <150 µm were picked for Nd isotope analysis between 28.6 and 29.935 mbsf of ODP Site 610B. No oxidative-reductive leaching procedure was employed, and this approach has been demonstrated to be suitable for extracting bottom water Nd isotopic compositions (Wu et al., 2015). The cleaning procedure and purification of Nd were carried out in a class 100 clean laboratory using ultrapure reagents. The foraminifera shells were crushed between two glass slides to open chambers, and the calcite fragments were ultrasonicated for 1 min in Milli-Q water before pipetting off the suspended particles. This step was repeated until the water was clear and free of clay particles. Samples were inspected under a binocular microscope to ensure that all sediment particles had been removed before they underwent weak acid leaching for 5 min in 1 ml 0.001 M HNO_3 with ultrasonication. After the cleaning step, samples were transferred into a 1.5 ml tube, soaked in 0.5 ml Milli-Q water, and dissolved using stepwise additions of 100 µl 0.5 M HNO_3 until the dissolution reaction was completed. The dissolved samples were centrifuged, and the supernatant was immediately transferred to Teflon beakers to prevent the leaching of any possible remaining phases. The solutions were then dried and Nd was purified using Eichrom TRU-Spec and Ln-Spec resins following the analytical procedure described in Copard et al., (2010). The $^{143}Nd/^{144}Nd$ ratios were measured using the Multi-Collector Inductively Coupled Plasma Mass Spectrometer (MC-ICP-MS Neptune$^{\text{Plus Thermo Fisher}}$) (PANOPLY's analytical facilities at the University Paris-Saclay, France) hosted at the *Laboratoire des Sciences du Climat et de l'Environnement* (LSCE, Gif-sur-Yvette, France). Sample and standard concentrations were matched at 10 to 15 ppb, and mass fractionation was corrected by normalising $^{146}Nd/^{144}Nd$ ratios to 0.7219, applying an exponential law. During the analysis, every group of three samples was bracketed with analyses of JNdi-1 Nd standard solution, which is characterised by certified values of 0.512115 ± 0.000006 (Tanaka et al., 2000). The analytical error reported for each sample analysis is based on the external reproducibility (2σ) of the JNdi-1 standard within a given session, unless the internal error was higher. The Nd isotopic composition is expressed as $\varepsilon_{Nd} = [(^{143}Nd/^{144}Nd)_{Sample}/(^{143}Nd/^{144}Nd)_{CHUR} - 1] \times 10{,}000$, where $(^{143}Nd/^{144}Nd)_{CHUR} = 0.512638$ represents the chondritic uniform reservoir (Jacobsen and Wasserburg, 1980).

3.6 Grain size analysis

We measured grain size distributions using a Mastersizer 3000 at the University of Galway, Ireland, School of Geography, Archaeology and Irish Studies. We applied a refractive index of 1.54 and an absorption index of 0.01, as recommended by *Malvern Panalytical*. We used ~1 g of dry bulk sediment; samples were pre-sieved at 1000 µm, and following Jonkers et al. (2015) we removed carbonates, organic matter, and opal, before measuring. Challenges associated with this method include air bubbles introduced to the optical cell within the Mastersizer during analysis, which can skew the results towards larger grain sizes. To alleviate this problem, we cut grain size distributions at 211 µm. Since 99% of sediments are below this size bin (Polakowski et al., 2021) cutting grain size distributions likely had no impact on sediments deposited by WTOW (i.e., silt ≤ 50 µm and clay ≤2 µm).

We then statistically unravelled grain size distributions into end-members using a non-parametric End-Member Analysis (Weltje, 1997) in AnalySize (v. 1.1.2) (Paterson and Heslop, 2015). A non-parametric approach estimates end-members from the dataset and does not rely on assumed knowledge of the distribution, i.e., the size distributions of the subpopulations are not known a priori and must be determined from the data itself (Paterson and Heslop, 2015;Chen and Guillaume, 2012). To ensure the datapoints adequately represent the end-members, we excluded specimens with a r^2 <0.99. The

https://doi.org/10.5194/cp-2023-101
Preprint. Discussion started: 4 January 2024

resulting end-members were assessed for their size, distribution and sorting. Well-sorted end-members in the silt-sized fraction were interpreted as current-sorted sediments, which preserve a bottom-water current speed signal (Prins et al., 2002), while poorly sorted end-members including sand and gravel were interpreted as representing IRD.

3.7 X-Ray Fluorescence analysis

X-Ray Fluorescence (XRF) analysis was performed at the Integrated Ocean Drilling Program, Bremen Core Repository, in Germany on DSDP Core 94-610A (0–38 mbsf) and 610B (24–34 mbsf). Data were collected every 0.5 cm down-core with a slit size of 5 mm using a generator setting of 10 kV, 0.035 mA and a sampling time of 10s directly at the split core surface using an XRF Core Scanner III (Avaatech) that measures selected elements between Aluminium and Uranium. Calcium (Ca), and Titanium (Ti) are common elements observed in marine sediments that can be used as palaeoenvironmental tracers (Gebhardt et al., 2008;Van Rooij et al., 2007;Arz et al., 2001). Ca is primarily of biogenic origin (Solignac et al., 2011), and reflects the presence of calcium carbonate ($CaCO_3$) tests of foraminifers and coccolithophorids in the sediments (Rothwell, 2015). It is well-recognised that $CaCO_3$ records in the Atlantic are related to Glacial-Interglacial cycles, with higher $CaCO_3$ concentrations during interglacials (Balsam and McCoy Jr, 1987). Ca can also be sourced from detrital material but this is most relevant in near-shore environments (Rebolledo et al., 2008) or in the IRD Belt (Ruddiman, 1977) during North Atlantic Heinrich events (Hodell et al., 2008). Ti is primarily terrigenous sourced and forms the detrital load (Haug et al., 2001). Here we use the log(Ti/Ca) as a proxy for evaluating relative variations in lithogenic/biogenic content (Piva et al., 2008).

4 Chronology

The fundamental aim of age modelling is to construct meaningful time series with age-depth relationships and report the associated errors (Breitenbach et al., 2012;Trachsel and Telford, 2017). The robustness of any age model depends on the number of fixed dates and the associated uncertainties (Telford et al., 2004). Astronomical tuning is a commonly used tool to build age models on Pleistocene sediment records (Clemens, 1999). Typically, sections are tuned to the LR04 benthic $\delta^{18}O$ stack record by Lisiecki and Raymo (2005) based on 65°N June insolation values. The age model for site 610B was constructed using continuous 0.5 cm resolution XRF analysis performed on DSDP sites 610A and 610B for the past 500 ka. The chronology of MIS 11 was further constrained using $\delta^{18}O$ values picked throughout the core. These $\delta^{18}O$ measurements were tuned to the benthic $\delta^{18}O$ record of the well-dated Ocean Drilling Project (ODP) site 980 (McManus et al., 1999), and its LR04

https://doi.org/10.5194/cp-2023-101
Preprint. Discussion started: 4 January 2024

Climate of the Past
Discussions

chronology, which has an uncertainty of ±4 ka BP (Lisiecki and Raymo, 2005). For a detailed description of tie points used to constraint site 610B over MIS 11, please consult Holmes et al. (2022) and Figure 3. Here, we add a further tie point at 29.58 mbsf (Figure 3) by linking the mid-interglacial maximum Np % from site 610B to the mid-interglacial peak in Np % from the well-dated site 983 (Barker et al., 2015).

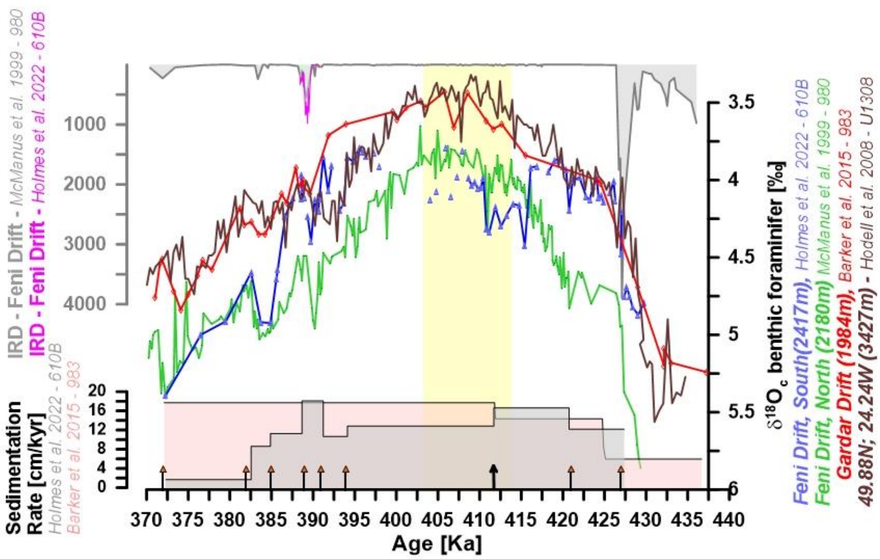

Figure 3. Age Model modified from Holmes et al. (2022). IRD counts from DSDP 610B (pink) and ODP 980 (grey) from the Feni Drift; $\delta^{18}O$ benthic foraminifera records from DSDP 610B (blue), ODP980 (green, and ODP 983 (red), IODP 303-U1308 (brown) corrected by 0.63 ‰. Sedimentation rates for DSDP 610B (grey) in cm.kyr^{-1} are adjusted for the additional tie point used in this study (black arrow). Orange arrows show tie points used in Holmes et al. 2002 and in this study. Also shown are sedimentation rates for ODP 983 (light pink). The yellow band marks the dataset shown here.

We acknowledge that in doing so we assume that the associated cooling of the 412-ka event occurred simultaneously across the subpolar North Atlantic. However, we believe that this approach is justified since most records (surface and deep-water) from the North Atlantic Region place the main signal of the ~412 ka event at 411.7 (±0.7) ka (Table 1). Further, we note that the duration of the surface cooling observed in records near site 610B (e.g., sites 980, U1314, 983, M23414 (TEX_{86})) is similar (0.4-0.9 ka) regardless of the age model used. Considering the short duration of the 412-ka event, <1 ka, and the uncertainties for chronologies based on $\delta^{18}O$ curves it would not be possible to assess the regional progression (if there was one) for the event with or without tie points between chronologies. With the inclusion of this additional tie point, the event occurred at 411.9 ka in core 610B, and the presented record here covers the period from 414.3-403.4 ka and sedimentation rates within this period correspond to ~82 years per cm.

Table 1: The event in surface and deep-water and the corresponding ages in the North Atlantic

https://doi.org/10.5194/cp-2023-101
Preprint. Discussion started: 4 January 2024

Surface water

Site	*Latitude*	*Longitude*	*Age (ka)*	*Depth (m)*	*Proxy*	*Reference*
ODP 983	60°4 N	23°6 W	411.8	1984	Np coiling ratio	Barker et al. (2015)
U1305	57°29 N	48°32 W	413.2	3459	Pf %	Irvali et al. (2020)
U1314	56°21 N	27°53 W	412	2820	Pf %	Alonso-Garcia et al. (2011)
ODP 980	55°29 N	14° 42 N	~411.1*	2179	Np %	Oppo et al. (1998)
M23414	53°32 N	20°17 W	411.3	2196	TEX_{86}	Kandiano et al. (2017)

Deep-water

Site	*Latitude*	*Longitude*	*Age (ka)*	*Depth (m)*	*Proxy*	*Reference*
U1305	57°29 N	48°32 W	411.6	3459	Ebf δ13C	Galaasen et al. (2020)
ODP 980	55°29 N	14° 42 N	~410.9*	2179	Ebf δ13C	McManus et al. (1999)
U1308	49°87 N	24°23 W	411.6	3427	Ebf δ13C	Hodell et al. (2008)

Pf – Planktonic foraminifera; Ebf – Epifaunal benthic foraminifera, *ODP Site 980 on the LR04 age model

To ensure an objective assessment of climate transitions for each data series (log(Ti/Ca), log(EM2/EM3), and MAT derived SST) presented here, we applied a Ramp function using the Fortran 77 program, RAMPFIT (Mudelsee, 2000). This is a statistical programme that uses Brute-force to estimate the unknown onset and end of a time interval by weighted least-squares regression to determine the best fit. Following Tibshirani and Efron (1993) we use a bootstrap simulation of 200 resamples to estimate the uncertainty of the results (Table 2). To determine the ramps objectively the search interval (x_1, x_2) was set as far apart as possible but before the next shift in climate state. This enabled the programme to statistically determine the most significant ramp for the onset, duration, and recovery for each dataseries. All search intervals are shown in Table 2.

Table 2: Rampfit for each proxy. Log(Ti/Ca) = lithogenic/biogenic variations, SST = Sea Surface Temperature, WTOW = Wyville-Thomson Overflow Water. Rampfit is an autoregressive model used to describe time-varying natural processes that accurately quantify transitions (Mudelsee, 2000). SE = standard error.

Dataset	**Interval**		**Ramp 1**	**SE**	**Ramp 2**	**SE**	**Duration**	**SE**
XRF Log(Ti/Ca)	412.23	415.5	412.68	0.24	414.58	0.22	1.9	0.39
	410.96	412.68	411.99	0.02	412.29	0.01	0.3	0.03
	410.03	411.99	410.69	0.23	411.08	0.23	0.39	0.4
	410.69	409.6	409.83	0.09	410.03	0.08	0.2	0.15
	409.83	408.23	408.62	0.17	409.75	0.14	1.13	0.26
	408.62	404.18	404.3	0.15	407.45	0.15	3.16	0.23
	404.3	400	401.88	0.8	404.26	0.7	2.38	1.19
WTOW	410.3	414.28	411.9	0.28	412.86	0.45	0.96	0.66
	408.12	411.9	410.1	0.55	410.3	0.54	0.2	0.67
	403.4	410.1	406.01	1.62	410.1	1.39	4.09	1.76
SST	411.66	414.28	411.9	0.34	412.62	0.36	0.72	0.44
	409.91	411.9	411.27	0.24	411.9	0.1	0.62	0.26

https://doi.org/10.5194/cp-2023-101
Preprint. Discussion started: 4 January 2024

	409.13	411.27	409.52	0.23	409.91	0.43	0.39	0.5
	403.4	409.51	406.4	0.87	409.32	0.68	2.92	1.27
	413.85	408.90	412.11	0.71	412.17	0.56	0.06	0.83
δ¹³C	412.11	405.74	408.86	0.97	408.90	0.99	0.04	0.99
	4.08.90	403	405.47	0.50	405.74	0.74	0.27	0.93

5 Results

5.1 X-Ray Fluorescence (XRF) and Ice-Rafted Debris (IRD)

At 412.29 (±0.01) ka the contribution of lithogenic versus biogenic (e.g., log(ti/Ca)) input sharply increases over 0.3 (±0.03) ka (Figure 4). Terrigenous input remains elevated for another 0.39 (±0.40) ka before decreasing towards a mid-event plateau. A second maximum in terrigenous input occurs at 409.75 (±0.14) ka. Thereafter, values decrease to pre-event values by 404.30 (±0.15) ka. The overall structure of the time series is best described by a two-step event. IRD abundance is relatively low throughout the record, fluctuating between 2.7 and 119.6 grains/g. Nevertheless, the overall structure between the XRF and IRD

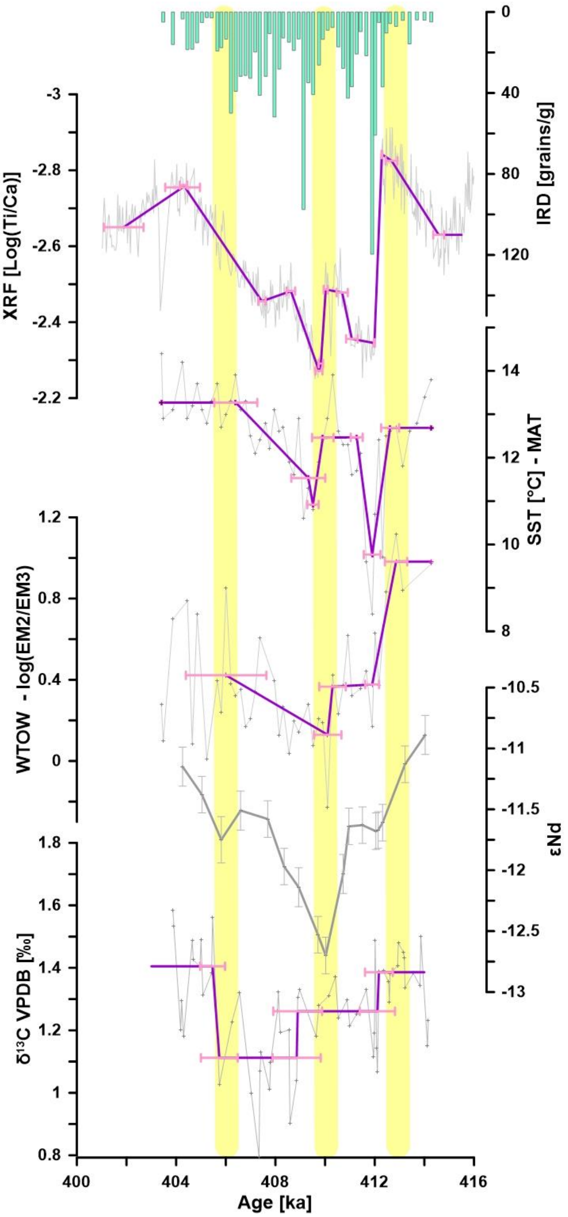

Figure 4: Results for MIS 11 proxy records from site 610B. From top to bottom. IRD >150 µm (#/gram) [green]; Log ratio of Ti/Ca, log(Ti/Ca), as a proxy for variations in lithogenic/biogenic inputs [purple]; SST [red], Log ratio of EM2 and 3, log(EM2/EM3), as a proxy for deep-water flow strength (WTOW) [blue]. Raw data for log(Ti/Ca), SST and WTOW, shown by faded line. Rampfit, an autoregressive model that quantifies climate transitions (Mudelsee, 2000), is shown in bold lines, with errors shown by horizontal bars.

https://doi.org/10.5194/cp-2023-101
Preprint. Discussion started: 4 January 2024

Climate of the Past
Discussions

records is similar with two distinct maxima centred at 411.90 and 409.52 ka, placing the maxima within the periods of maximal lithogenic input, as inferred from the XRF record (Figure 4).

5.2 Sea surface temperatures (SST) and foraminifera abundances (%)

The two-step event structure is also evident in the MAT-derived SST reconstruction (Figure 4). Before the event, between 414.3 and 412.62 (±0.36) ka, SST values describe a period of persistent warmth (e.g., 11.8-13.8 °C). Over the same period, foraminifer assemblages show relatively high abundances (Figure 5) of transitional species (i.e., *G. bulloides, G. glutinata*), and an enhanced influence of the subpolar species, *N. incompta*, reaching maximum abundance, forming almost 50% of the total assemblage, just before the first cooling event at 412.62 (±0.36) ka. The first drop in SST of ~3.0°C from 12.7°C to 9.77°C occurred between 412.62 (±0.36) and 411.90 (±0.10) ka. A distinct shift from subpolar/transitional species during this period with minimum values of *G. inflata* (4.5%), a sharp reduction in *G. bulloides* (10.2%) and *N. incompta* (39.8%) indicates a reduced influence of warm, saline Atlantic Waters during this time. SSTs recovered to 12.5°C before decreasing a second time to 10.9°C at 409.51 (±0.23) ka. This second cooling is concurrent with an increase of Np and an

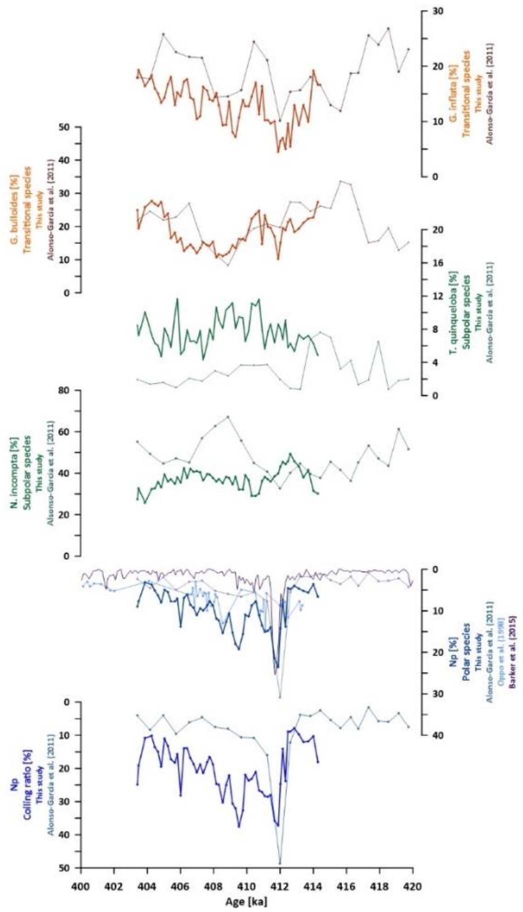

Figure 5 The evolution of planktonic foraminifera during peak MIS 11 conditions. From top to bottom, the relative abundances of G. *inflata* (transitional) [orange site 610B], [brown site U1314], *G. bulloides* (transitional), [orange site 610B], [brown site U1314], *T. quinqueloba* (subtropical), [dark green 459 610B], [light green site U1314] *N. incompta* (subtropical), [dark green site 610B], [light green site U1314], Np – note reversed axis (polar), [dark blue site 610B], [light blue site U1314], [baby blue, site ODP 980], [deep purple, site ODP 983] and Np coiling ratio (%) – note reversed axis, [dark blue site 610B], [light blue site U1314]. NOTE: OPD site 980 data have been updated to the LR04 age model. We exclude site U1305 data as the hydrographic setting is so different that the values do not easily plot with the data from the eastern North Atlantic. Please refer to the original publication for details (Irvalı et al., 2020).

https://doi.org/10.5194/cp-2023-101
Preprint. Discussion started: 4 January 2024

increase in the Np coiling ratio to 37.6%. From then onwards SST slowly recovered, reaching higher than pre-event values by 406.40 (±0.87) ka. Maximum values of 14.4°C occur towards the end of our record at 403.40 ka. Both Np % and the Np coiling ratio track the two-step nature of the event as seen in the XRF and SST records in terms of range of change and timing. The strong agreement between IRD, SST, and XRF (Figure 4) supports the interpretation of the log(Ti/Ca) record as a climate indicator, reflecting relative changes between IRD (i.e., lithogenic content) and climate (i.e., high $CaCO_3$ production during warmer climates).

5.3 Grain size analysis

Our grain size analysis indicates the sediments are adequately described by three end-members, one IRD (end-member 1; EM1), and two overflow (end-members 2 and 3; EM2 and EM3), inferred from both the R^2 and angular distance (θ) goodness-of-fit statistics ($R^2 = 0.253$, θ = 2.3°) (see also Supplement Figure S1). The well-sorted EM2 and EM3 consist primarily of clay and fine silt sediment with mean grain sizes of 5.21 µm and 9.86 µm, respectively, characteristic of sediments sorted by bottom-water currents (Figure 6). The log ratio of EM2 and EM3 (log(EM2/EM3)) is used as a proxy for WTOW flow strength in the Rockall Trough (Prins et al., 2002). This ratio describes the relative increase in grain size of EM2 over EM3 and thereby a decrease in values infers a decrease in flow strength (Figure 4 and 6). EM1 is poorly sorted and is composed of 49.4 % clay, 50.3 % silt, and 0.32 % sand (Figure 6). The relatively high proportion of clay and silt in EM1 suggests that EM1 most likely represents IRD (Andrews, 2000;Jonkers et al., 2012;Nürnberg et al., 1994). The highest contribution of the two, well-sorted end-members (log(EM2/EM3)) occurs in the oldest part of our record between 414.28 and 412.86 (±0.45) ka when IRD is low. At 412.86 (±0.45)

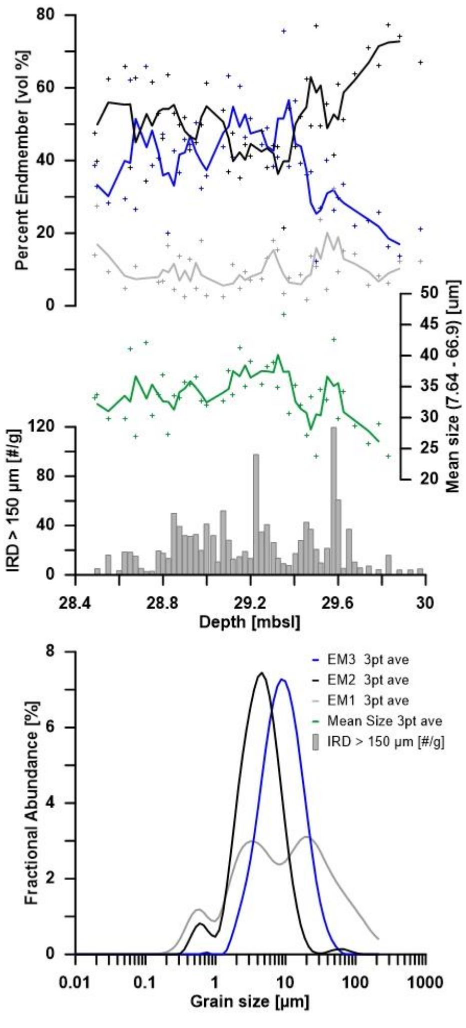

Figure 6 Grain size analysis. From the bottom up: The bottom graph shows the grainsize distribution of the main endmembers EM1(grey), EM2(black), and EM3(blue). This is followed by IRD >150 (grey bars), the mean grainsizes (7.64-66.9 µm) for each sample, and the proportion of each endmember (EM1-grey, EM2-black, and EM3-blue) plotted versus depth.

https://doi.org/10.5194/cp-2023-101
Preprint. Discussion started: 4 January 2024

Climate of the Past Discussions

ka WTOW begin to decrease over 0.96 (±0.66) ka before stabilising between 411.90 (±0.28) and 410.30 (±0.54) ka. At 410.30 (±0.54) ka a second decrease in values occurs over 0.20 (±0.67) ka. Thereafter, overflows slowly recover but remain below pre-event values and are variable until the end of the record.

5.4. ϵNd and stable isotopes ($\delta^{18}O$ and $\delta^{13}C$)

At 414 ka ϵ_{Nd} values are most radiogenic at -10.9 ± 0.2. This is followed by a decrease to less but stable ϵNd values of -11.6 ± 0.2 between 412.31 and 410.92 ka. After 410.92 ka, ϵ_{Nd} values decreased a second time to reach the lowest value of -12.7 ± 0.15 at 410.02 ka. Thereafter ϵ_{Nd} values increased steadily until 407.68 and then again after 405.04 ka to reach -11.15 ± 0.15 at the end of the dataset (Figure 4). We note that due to the limited sample set, we were not able to perform rampfit functions to support the interpretation of the onset and recovery of the event with statistics in the ϵ_{Nd} dataset. Both $\delta^{18}O$ and $\delta^{13}C$ values were high at 3.9-4.0 ‰ and 1.3-1.5 ‰ respectively at 414 ka. Following a two-step pattern $\delta^{13}C$ decreased first to 1.26 ‰ between 412.16 ± 0.56 and 408.89 ± 0.99 ka followed by a second decrease to 1.12 ‰ between 408.86 ± 0.97 and 405.74 ± 0.74 ka. We note that variability is high in this interval and notably $\delta^{13}C$ values decrease to reach low values of 0.79 ‰ at 407.34 ka. The recovery to more enriched $\delta^{13}C$ values began after 405.47 ± 0.50 ka to reach 1.41‰ which are higher than pre-event values. $\delta^{18}O$ values steadily decreased by 0.5-0.7 ‰ from 3.9-4.0 to 3.3-3.4 ‰ over the 10-ka analysed here.

6 Discussion

6.1. The 412-ka event

Sea surface temperature records across the Northeast Atlantic, from the Gardar Drift to the Rockall Trough (e.g., sites 983, U1314, M23414, 980 and this study), record warm Holocene-like sea surface conditions before ~412 ka (Kandiano et al., 2012). However, between 412.62 (±0.36) and 411.90 (±0.10) ka sea surface data at site 610B shows an increase in Np abundance (4.8 to 23.5%) and a drop in SST of 3.0°C from 12.7°C to 9.77°C (Figure 4 and 5). Similarly, at sites 983, 980, and U1314 polar species increase at ~412 ka (Figure 5). At site M23414, both mid-depth (TEX_{86}) and sea surface records (Alkenone) also record a decrease in SST of 5.7°C in TEX_{86} and 1.5°C in Alkenone SST at 412 ka (Figure 7) (Kandiano et al., 2017a). However, the event is absent in planktonic assemblage-based SST records at the same site (Kandiano and Bauch, 2007) which is puzzling given the strong regional signal for the event. A review of the methods used for SST reconstructions in Kandiano and Bauch (2007) reveals that the foraminifera - based SST dataset was derived by combining and averaging three different methods to infer summer SSTs using: Transfer Function Technique (TFT; Imbrie and Kipp (1971), MAT;

https://doi.org/10.5194/cp-2023-101
Preprint. Discussion started: 4 January 2024

Climate of the Past
Discussions

Prell (1985)) and Revised Analogue Method (RAM; Waelbroeck et al. (1998)). Using the average may have smoothed out the event in the resultant SST data series.

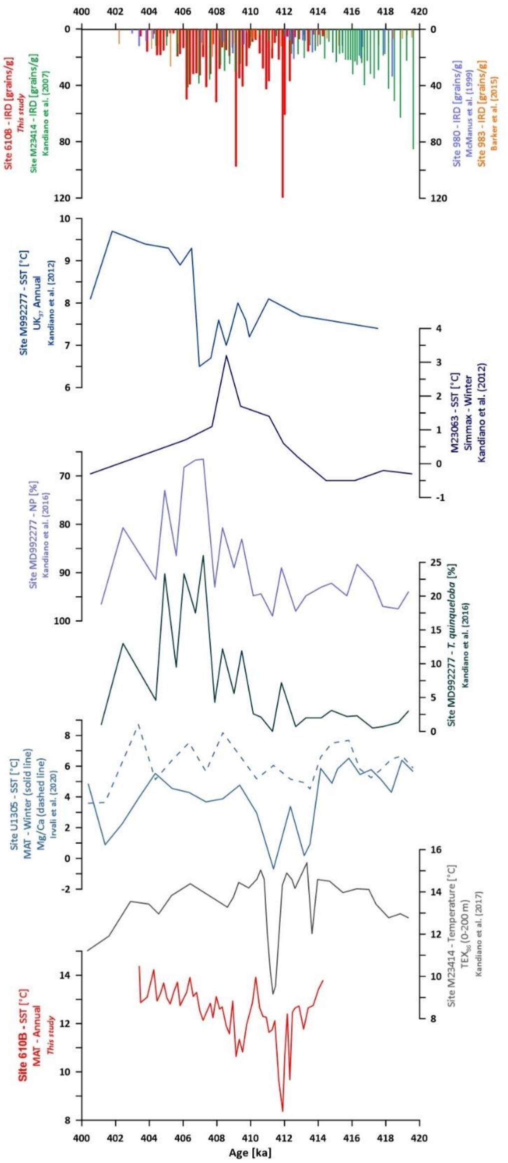

Further west on the Eirik Drift warm conditions also prevailed just downstream of the East Greenland Current (EGC) (e.g., site U1305, Figure 2) with Np coiling ratios of 41.9-83.7% and SST near 10°C from 420 ka until ~413.5 ka (Figure 7) (Irvalı et al., 2020). Unlike reconstructions from the Northeast Atlantic, these data provide evidence for a much warmer sea surface climate when compared to early Holocene and modern core top (e.g., 7.7°C) values downstream of the EGC (Irvalı et al., 2020). This long period of warmth is interrupted by a two-step cooling event of 7.2°C, from 10°C down to 2.8°C between 413.2-411.4 ka (Irvalı et al., 2020) (Figure 7). The cooling is coeval with Np abundance and coiling ratio reaching 96.5% and 100% respectively, and occurred over approximately 0.8 ka (Irvalı et al., 2020). On the Gardar Drift (site U1314) the Np % increase is also of high-magnitude (from 3.8% to 48.6%) and occurs over 2 samples representing 1.22 ka (Alonso-Garcia et al., 2011). We note that the duration of these transitions is limited by the resolution of the respective archives and are thus maximum estimates.

Figure 7: Surface hydrographic conditions during MIS 11. IRD grains/g records sites: site 610B [red] this study; site 980 [blue] (McManus et al., 1999); site M23414 [green] (Kandiano and Bauch, 2007) on the updated age model from Kandiano et al. (2017b) and site 983 [orange] (Barker et al., 2015). SST [°C]/ foraminifera assemblages [%] from top to bottom: Annual SST (UK_{37}), site MD992277 (Kandiano et al., 2012); Winter SST (Simmax), site M23063 (Kandiano et al., 2012); % *N. pachyderma* – Np – note reversed axis, site MD992277 (Kandiano et al., 2016); *T. quinqueloba*, site MD992277 (Kandiano et al., 2016); SST (Mg/Ca), site U1305 [dashed line], Winter SST (MAT) site U1305 [solid line], (Irvalı et al., 2020); SST TEX_{86} (0-200 m) site M23414 (Kandiano et al., 2017b); MAT SST, site 610B (this study).

https://doi.org/10.5194/cp-2023-101
Preprint. Discussion started: 4 January 2024

In the Nordic Seas, the 412-ka event trajectory seems to have been reversed (Figure 7). During early MIS 11 (e.g., 424-412 ka) evidence for cold and fresh surface waters in the Iceland and western Norwegian Sea is widespread. For example, at site M23352 in the North Iceland Basin (Figure 2), continuous IRD during early MIS 11 (Helmke and Bauch, 2003), indicate that cold waters dominated this core site until ~407.5 ka. Similarly, at site M992277 (sometimes referred to as PS1243) located in the central Nordic Seas (Figure 2), high percentages of Np (81-99%) imply cold conditions until ~407 ka (Kandiano et al., 2012). Further east, at site M23063, cold temperatures prevailed until ~412.8 ka (Kandiano et al., 2012). A comparison of foraminifera abundance-derived temperatures between the first half of MIS 11 and the early Holocene (11-5.5 ka) at site M23063 illustrates the sharp difference between the much warmer Holocene (4.12°C) and cold early MIS 11 (0.1°C), emphasising the unique hydrographic conditions in the central Nordic Seas at the time (Kandiano et al., 2012). These datasets also illustrate that cold waters reached much further east in the central Nordic Seas than during the early Holocene (Doherty and Thibodeau, 2018; Kandiano et al., 2017b). Multiple studies hypothesise that continuous background melting of the GIS especially south of 69°N contributed to these cold sea surface conditions until 412 ka (de Vernal and Hillaire-Marcel, 2008; Reyes et al., 2014b; Robinson et al., 2017b; Robinson et al., 2012; Willerslev et al., 2007). Mid-way through MIS 11, SSTs transition to warmer more Holocene-like conditions. The exact timing for the transition from cold to warmer SSTs is difficult to determine given the low resolution of records from the Nordic Seas and chronological constraints, however, the general timing and trends in surface records appear to coincide with the cold event in the subpolar North Atlantic at ca 412 ka.

What was the cause for the sudden sea surface cooling across the subpolar gyre at 412 ka? The faunal assemblage changes and inferred SST cooling of 7°C at site U1305, describe a rapid transition from Atlantic to Polar Waters immediately downstream of the EGC (Figure 5). Specifically, the decrease of *T. quinqueloba* while Np % is increasing is indicative of the passage of the SAF and Polar Front over the site (Alonso-Garcia et al., 2011;Mokeddem et al., 2014). This rapid transition in foraminifera assemblages is also recorded at sites U1314 and 983 albeit at lower magnitudes invoking an eastward progression of cold and potentially freshwater, together with the SAF, across subpolar latitudes during the event.

A potential source of ice or cold/freshwater could have come from residual continental Ice during early MIS 11. Indeed, most estimates of sea level rise following Termination V (Rohling et al., 2010; Elderfield et al., 2012; Grant et al., 2014; Shakun et al., 2015; Spratt and Lisiecki, 2016; Giaccio et al., 2021), agree that about 50–80 m SLE remained present in ice sheets near the start of MIS 11c due to

https://doi.org/10.5194/cp-2023-101
Preprint. Discussion started: 4 January 2024

weak caloric summer insolation at 65˚N at 424 ka. By 412 ka estimates still assume the presence of between -38.7 to +3.9m SLE of continental Ice (Sprat and Lisiecki et al. 2016, Grant et al. 2014, Shakun et al. 2015, Elderfield et al. 2012). These estimates invoke the presence of several Greenland equivalent size Ice sheets present at 412 ka. However, there is little geologic or terrestrial evidence to support the presence of continental ice of this scale at high northern latitudes by 412 ka. For example terrestrial palaeoclimate records from Europe (Tzedakis et al., 1997;Reille et al., 2000;Tzedakis et al., 2006;Ashton et al., 2008;Preece et al., 2007;Nitychoruk et al., 2005) and Siberia (Prokopenko et al., 2010;Melles et al., 2012;SHICHI et al., 2009) provide evidence for increased forestation at high northern latitudes replacing tundra or frozen soils in Eurasia, driven by a lengthening of the growing season during the obliquity maximum at 416 ka. Model simulations further suggest that the decrease in summer sea ice at this time led to warming feedback during the winter at high Northern latitudes amplifying the insolation-induced warming (Kleinen et al. 2014). Similarly, pollen-based reconstructions (Melles et al., 2012;Prokopenko et al., 2010;SHICHI et al., 2009;Desprat et al., 2005b;Nitychoruk et al., 2005) support warmer than present summers and winters in the High Arctic Region throughout MIS11 until at least 405 ka.

A recent investigating into the retreat of the Laurentide Ice Sheet (LIS) following the glacial Termination of MIS 12 (e.g., T5) also shows that the LIS would have been mostly deglaciated with the Hudson Bay Ice Saddle collapse at 419 ± 4.7 ka (Parker et al., 2023). There is a possibility that ice remained on land (e.g., Keewantin Ice Dome and/or Quebec-Labrador Ice Dome) until ca 405 ± 4.7 ka (Parker et al., 2023) contributing to background melting via Hudson Bay from 419-405 ka. While background melting is possible, the relatively low IRD input throughout the North Atlantic region following the Hudson Bay Ice Saddle collapse and during the 412-ka event make it unlikely that a collapse of marine-terminating ice shelves or glaciers from the LIS was involved in cooling the subpolar North Atlantic. Indeed, IRD of 2.7-119.6 grains.g^{-1} at site 610B throughout the event are comparable to Holocene values of 4.7-113.9 grains.g^{-1} recorded from the Feni drift at site 980 (McManus et al., 1999). Similarly, IRD counts from Gardar Drift at site 983 (Barker et al., 2015) and from Eirik Drift at site U1305 (Irvalı et al., 2020) are also low and comparable to Holocene values. Thus, delivery of Icebergs remained low during the 412-ka event suggesting a distal source for calving icebergs at best. Finally, if background melting via Hudson Bay persisted over the 419-405 ka period, we note that it does not seem to have significantly impacted subpolar North Atlantic SSTs given the widespread Holocene-like SSTs across mid-latitudes before the 412-ka event.

https://doi.org/10.5194/cp-2023-101
Preprint. Discussion started: 4 January 2024

Another possibility for the presence of continental Ice may be an ice sheet northwest of Greenland restricting the Canadian Arctic Archipelago until 412 ka. If so, this could have channelled all freshwater exports via Fram Strait into the Nordic Seas (Lofverstrom et al., 2022) and thereby contributed to the anomalously cold SST observed from the Nordic Seas until 412 ka. Once open, Arctic freshwater would have been channelled south via both Baffin Bay and Fram Strait reducing freshwater export into the Nordic Seas. We note that this scenario could explain the warming trend observed in the Nordic Seas around the 412-ka mark. However, the presence of land ice in the Canadian Arctic Archipelago until 412 ka is difficult to reconcile with the evidence for high latitude warming from terrestrial and modelling evidence and the full deglaciation of Camp Century (77.17°N 61.13°W) by 416 ± 38 ka. (Christ et al., 2023). Furthermore, while dating uncertainties are large, there is evidence that Camp Century remained fully deglaciated for at least 16 ka, which must precede the glacial inception at 397 ka and therefore 412 ka. Finally, models and terrestrial records indicate a completely ice-free southern and western Greenland, except for highly elevated areas, by 411 ka (Robinson et al., 2017b;Robinson et al., 2012). Low RSL estimates for early MIS 11 based on benthic foraminifera $\delta^{18}O$ records thus seem to stand alone against multiple lines of evidence suggesting that high northern latitudes were experiencing warmer climates and less ice. Nevertheless, we cannot rule out that land ice persisted and contributed to the event given the chronological uncertainties associated with palaeo records.

6.2 Deep-water response to the 412-ka event.

The leading hypothesis describing a strong AMOC during early MIS 11 posits that a strong density gradient between the subpolar North Atlantic and the Nordic Seas supported strong deep-water formation in the Nordic Seas (Kandiano et al., 2012;Doherty et al., 2021). Our data supports the presence of strong Nordic Sea deepwater production before 412 ka. First, grain-size inferred current velocities preceding the event are among the highest recorded throughout MIS 11 including the glacial inception (Holmes et al., 2022). Further, both $\delta^{18}O$ and $\delta^{13}C$ values are enriched at 3.9-4.0 ‰ and 1.3-1.5 ‰ respectively, indicating a strong nutrient-poor northern source of deep waters such as ISOW/WTOW from the Nordic Seas before the event (Figure 4). Similarly, the radiogenic ε_{Nd} signal of -10.89 supports a strong influence of ISOW/WTOW (−10.3 ± 0.2) (Dubois-Dauphin et al., 2017) at the site (Figure 4). In combination with high WTOW flow endmembers, this supports vigorous export of NSDW via the Wyville-Thompson Ridge into the Rockall Trough before the 412-ka event.

Starting at 412.86 (±0.45) ka grain-size inferred current velocities describe a two-step decrease in flow strength. Considering the temporal uncertainties, this reduction in overflow is concurrent with the SST decreases at 412.62 (±0.36) ka. However, the higher resolution log(Ti/Ca) data records the change in surface ocean properties at a multi-centennial delay with respect to the overflows at 412.29 (±0.01)

https://doi.org/10.5194/cp-2023-101
Preprint. Discussion started: 4 January 2024

Climate of the Past
Discussions

ka. This delay occurs within uncertainties of the SST record but is significant compared to the overflows. This would suggest that there is a significant offset between the surface and deep-water response to the cooling event recorded at site 610B. In effect, this highlights that deep water circulation responds to cooling at subpolar latitudes before the eastward progression of cold water reaches the eastern North Atlantic.

Concurrent with the two-step decrease in WTOW flow estimates, ε_{Nd} values become less radiogenic reaching the lowest values of -12.7 ± 0.15 at 410.02 ka (Figure 4). Together, these data suggest a decrease in flow strength and a decrease in ISOW/WTOW contribution, replaced by either the less radiogenic eNd Lower NADW (−12.1 ± 0.2 and 13.1 ± 0.2) or LSW (−13.4 ± 0.3 and −14.0 ± 0.3) (Dubois-Dauphin et al., 2017;Lambelet et al., 2016) (Lambelet et al., 2016;Dubois-Dauphin et al., 2017) at site 610B. A larger contribution of LNADW or LSW is more likely than a larger contribution of Mediterranean Overflow Water (MOW) or Southern sourced Ocean Waters (SOW) at this time because both have an ε_{Nd} signature of -11, which is too radiogenic to explain the excursion observed in the data.

Following the lowest flow rates and reduced WTOW contribution at 410.02 ka benthic foraminiferal $\delta^{18}O$ and $\delta^{13}C$ values at 610B at site 610B decrease (see also Supplement Figure S2), suggesting a possible increased influence of SOW, LDW or/and LSW at site 610B than before the event. This is also mirrored in the paired benthic $\delta^{18}O$ and $\delta^{13}C$ values from the Eirik Drift at site U1305 (Galaasen et al., 2020) and at site U1308 (Hodell et al., 2008) located to the southwest of the Rockall Trough. At Eirik drift the event is marked by a drop in benthic $\delta^{13}C$ values of ca. 0.6 ‰ from 0.80 to 0.20 ‰. This decrease, while smaller, is reminiscent of the 1 ‰ decrease observed during the 8.2 ka event when glacial Lake Agassiz drained into the subpolar North Atlantic during the early Holocene (Kleiven et al. 2008). Kleiven et al. 2008 suggested that this decrease in benthic $\delta^{13}C$ values describes the replacement of low-nutrient LNADW supplied by DSOW with a high-nutrient deep-water mass from a southern source (e.g., SOW) at the core site.

A shoaling and northwards extension of SOW into the Rockall Trough may also be a plausible response to the decrease in NSDW formation at 412 ka. Modern SOW is characterised by ε_{Nd} values near -11 (Dubois-Dauphin et al., 2017) and depleted $\delta^{13}C$ values of 0.0 - 0.2 ‰ (Eide et al., 2017). The return to more radiogenic ε_{Nd} values shortly after 410 ka while both WTOW flow speeds and $\delta^{13}C$ remain depleted/variable could therefore be linked to a larger contribution of SOW at site 610B rather than a rapid return of WTOW. A more northern influence of SOW during the event is also supported by a 0.6 ‰ drop in $\delta^{13}C$ from ca 1.1 to 0.5 ‰ at site U1308 (south of site 610B) (Figure 8). We note that no significant change in $\delta^{13}C$ is observed at the more northern site 980 over this timeframe, suggesting

https://doi.org/10.5194/cp-2023-101
Preprint. Discussion started: 4 January 2024

Climate of the Past
Discussions

that the northward extend of SOW was perhaps limited to the southern Rockall Trough. Alternatively, the deeper location of site 610B relative to site 980 (ca. 300m) may describe the depth boundary of SOW influence during the event.

By 405.74 ka benthic carbon isotopes return to more enriched values. This trend is also seen at sites U1308 and U1305 (Galaasen et al., 2020, Hodell et al. 2008) (Figure 8). ε_{Nd} values return to ca. -11.15 altogether suggesting a return of WTOW at site 610B, however, the highly variable nature of flow speeds in our WTOW flow record suggests that southward flow might have been intermittent at this time – perhaps similar to modern observations (Johnson et al., 2017). The slow recovery of WTOW current velocities seems to coincide with the slow retreat of cold waters towards the SPG. For example, at site 610B SSTs only reach pre-event values by 406.40 (±0.87) ka and warmest SST by the end of the dataset at 403.40 ka. Similarly, Np % decreases slowly across the SPG (e.g., sites U1314, U1305, 980) to reach pre-event values by ~406 ka (Alonso-Garcia et al., 2011;Irvalı et al., 2020;Oppo et al., 1998). We also note that the variability and continued presence of some minor IRD at site 610B coincides with lower benthic $\delta^{13}C$ throughout the record, suggesting a relationship between continued iceberg rafting and deep ventilation until 405.74 ka. The faster recovery observed in $\delta^{13}C$ values shortly after the event at sites 980 and M23414, may again be linked to the shallower depth of both sites relative to site 610B, and delimit the varying depth boundaries of water masses during the perturbation.

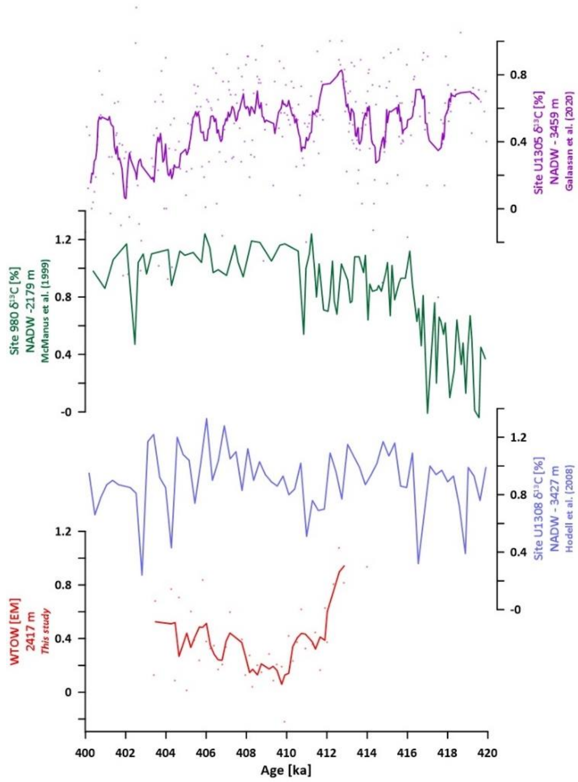

Figure 8: Deep-water records from North Atlantic Region. Top to bottom, $\delta^{13}C$ – water mass proxy – site U1305 [purple] (Galaasen et al., 2020); site 980 [green] (McManus et al., 1999); site U1308 [light blue] (Hodell et al., 2008);, WTOW grain size analysis– deep-water strength proxy site 610B [red] (this study). NOTE: OPD site 980 data updated to the LR04 age model.

6.3. Climate forcing and Ocean-Atmosphere teleconnections.

A strong AMOC seems at odds with the western Nordic Seas covered by meltwater, especially since strong deep-water formation in the Nordic Seas requires Atlantic inflow and open-ocean convection (Eldevik et al., 2014). However, evidence for a strong AMOC particularly coinciding with the peak in obliquity (Kessler et al., 2020) at 416 ka is supported by several model simulations (Rachmayani et al., 2017) and palaeoceanographic reconstructions from the North (Galaasen et al., 2020) and South Atlantic (Dickson et al., 2009;Dickson et al., 2010). Revisiting the location and datasets used to infer the cooling in the Nordic Seas may allow us to reconcile model simulations and observations. The three sites from the Nordic Seas covering MIS 11 are located in the Iceland Sea and the western Norwegian basin between 65-70°N. Today these sites are mostly influenced by the Jan Mayen Current and the East Icelandic Current recirculating Arctic Waters from the EGC in the Iceland Sea Gyre. We also note that the datasets inferred from these sites are based on foraminifera and Alkenones, both known to represent a seasonally constrained summer signal especially at these high northern latitudes (Fraile et al., 2009;Kretschmer et al., 2018;Bendle et al., 2005).

A series of time slice simulations across MIS-11 suggest that boreal summers were particularly warm around Western Greenland, notably over the Canadian Arctic Archipelago and the high latitudes of the Atlantic sector for a period of at least 10 ka from 418-408 ka leading to weakened high latitude winds and the emergence of a single, unified midlatitude jet stream across the North Atlantic sector during boreal summers (Crow et al., 2022). Similarly, Rachmayani et al. (2017) simulate a negative southerly wind anomaly along the east Greenland margin centred over the Denmark Strait for MIS 11 in comparison to MIS 5e. If correct this more zonal and weaker circulation pattern might have led to reduced export of cold waters out of the Nordic Seas on a seasonal basis. Reduced meridional wind forcing during MIS11 summers (e.g., Crow et al. 2022) and an enhanced seasonal recirculation of meltwaters in the Iceland gyre (Le Bras et al., 2018) may therefore be plausible mechanisms explaining the “cool” Nordic Seas and “warm” subpolar North Atlantic signals.

Interestingly, the negative southerly wind anomaly centred over the Denmark Strait for MIS 11 is also associated with an increased advection of salt from the south to the eastern North Atlantic (Rachmayani et al., 2017) supporting strong NADW formation. Enhanced northern salt advection and strong NADW formation during times of enhanced GIS melting have also been simulated in response to RCP8.5 emission scenarios (Berk et al., 2021). Where the freshwater-induced weakening of Labrador Seawater formation is compensated by a strengthening of NSDW formation similar to observations made in (Wood et al., 1999;Swingedouw et al., 2013). Mechanistically, it is the weakened subpolar gyre that leads to a shift of the North Atlantic Current and subpolar-subtropical gyre

https://doi.org/10.5194/cp-2023-101
Preprint. Discussion started: 4 January 2024

boundary, with the subtropical gyre expanding and the subpolar gyre contracting (Swingedouw et al., 2013;Berk et al., 2021). Under this scenario, it is possible that Atlantic Waters reached the northern Nordic Seas pre-412 ka, perhaps in the form of a narrow boundary current along the Norwegian continental margin contributing to high latitude warming and deepwater formation while the Icelandic Sea remained cool as also observed during the early Holocene (Risebrobakken et al., 2011;Telesiński et al., 2022).

We cannot rule out that the collapse or melting of remnant continental ice caused the 412-ka event, however, the low IRD counts associated with the event do not support Ice rafting. Instead, we hypothesise that a change in the seasonal balance of freshwater export from the Nordic Seas into the North Atlantic via the Denmark Strait might have initiated a reorganisation of the freshwater distribution at polar/subpolar latitudes. This could have led to a shift of the subpolar-subtropical gyre boundary and thereby the northward advection of Atlantic Waters and cooling across the North Atlantic Region. The difference between the recirculation of polar waters and "freshwater hosing" scenarios, in which the thermohaline circulation weakens or collapses (Stouffer et al., 2006;Vellinga et al., 2008;Drijfhout, 2015), therefore appears to be linked to freshwater reaching the Nordic Seas via the Eastern North Atlantic (e.g., NAC). This has been hypothesised previously for future climate simulations (Berk et al., 2021) and demonstrated for glacial boundary conditions (Muschitiello et al., 2019) and the glacial inception following MIS11 (Holmes et al., 2022). We now show that similar freshwater (or sensitivity of thermohaline circulation) dynamics may have been in operation for full interglacial boundary conditions similar to our pre-industrial climate.

The evidence presented here highlights the sensitivity of NSDW formation to the reorganisation of freshwater across the polar/subpolar boundary and the movement of the subpolar-subtropical gyre boundary and therefore supports the recent hypothesis that high-magnitude variability of the AMOC may not require major additions or outbursts of freshwater (Galaasen et al., 2020). Instead, the reorganisation of Atlantic vs Polar waters at subpolar latitudes (Sgubin et al., 2017b) and thereby the density gradient across the SPG (Müller et al., 2015) and between the subpolar North Atlantic and the Nordic Seas (Jungclaus et al., 2006b) may determine high magnitude interglacial variability and strength in overturning (Olsen et al., 2008;Hansen and Østerhus, 2000;Østerhus et al., 2001;Mauritzen, 1996). For example, the variability in WTOW current velocities after the 412-ka event illustrates a higher sensitivity of the overflows to the weaker density gradient between the Nordic Seas and the subpolar North Atlantic modulated by a stronger east-west oriented SPG pushing the subpolar-subtropical gyre boundary and with-it icebergs/freshwater into the eastern north Atlantic.

https://doi.org/10.5194/cp-2023-101
Preprint. Discussion started: 4 January 2024

We note that state jumps (or hysteresis) in gyre circulation and exchange have also been found in simple (Born and Stocker, 2014) and coupled models (Born et al., 2013) and can be associated with a collapse in deep convection and reorganisation in AMOC geometry (e.g. where deep water is formed) (Sgubin et al. 2017).

7 Conclusion

Prolonged interglacial warmth during MIS 11 especially at high northern latitudes led to intensive background melting and the demise of continental ice sheets, including the southern and western Greenland Ice Sheets (GIS) by ~412 ka. Despite the addition of freshwater to the Nordic Seas, Deep-Water formation there remained strong, sustained by a strong density gradient between the Nordic Seas and the subpolar North Atlantic.

The abrupt reorganisation of freshwater into the Subpolar Gyre (SPG), and expansion into the eastern North Atlantic at 412-ka, reduced the density gradient between the Nordic Sea and the SPG and thereby the inflow of Atlantic Waters into the Nordic Seas. In addition, continuous freshwater export into the SPG may have further subdued deep-water flow in the western North Atlantic, for the remainder of the interglacial.

The evolution of surface and deep-water circulation described here sheds important insights on the sensitivity of deep-water formation in response to continuous background melting from the GIS during similar or warmer than present climate boundary conditions. Our examination reveals that the reorganisation between Polar and Atlantic Waters at subpolar latitudes is central mechanistically, not only for intermediate (Muschitiello et al., 2019), and low-ice (Holmes et al., 2022) boundary conditions but also for warm interglacial climates such as MIS 11 and the current Holocene.

Our findings demonstrate that the availability and/or rate (Lohmann and Ditlevsen, 2021) of freshwater reaching subpolar latitudes is modulated by non-linear atmosphere-ocean feedbacks (e.g., rate-induced tipping point), regardless of boundary conditions. This is crucial given current and projected GIS melting, and the estimated sensitivity of the AMOC to surface water buoyancy fluctuations (Smeed et al., 2014;Thornalley et al., 2018;Caesar et al., 2018;Bakker et al., 2016;Yu et al., 2016). This study concludes that continuous freshwater input alone is unlikely to inhibit NSDW formation and that a reorganisation of surface waters at subpolar latitudes is fundamental to overflow strength.

Data and materials availability

https://doi.org/10.5194/cp-2023-101
Preprint. Discussion started: 4 January 2024

All data needed to evaluate the conclusions in the paper are presented in the paper and/or the Supplementary Materials. Raw data will be made available in Pangaea upon publication.

Author contribution

The research and iCRAG-GSI Environmental Geoscience proposal was designed and managed by AM in collaboration with UN and CC. MC performed faunal counts, sediment size analysis, IRD counts, XRF scans, and data analysis and wrote the first draft of the manuscript. UN performed stable isotope analysis. CC and MMOC performed Nd analysis. AM wrote the final version of the manuscript with contributions from UN and CC.

Competing interests

The contact author has declared that neither they nor their co-authors have any competing interests.

Acknowledgements

We gratefully acknowledge the assistance provided by Arnaud Dapoigny and Louise Bordier during Nd isotope analyses.

Financial support

This research has been supported by the iCRAG-GSI Environmental Geoscience PhD Programme (17/RC-PhD/3481) awarded to AM and MMOC and the Galway Fellowship awarded to MC.

References

Aguiar, W., Meissner, K. J., Montenegro, A., Prado, L., Wainer, I., Carlson, A. E., and Mata, M. M.: Magnitude of the 8.2 ka event freshwater forcing based on stable isotope modelling and comparison to future Greenland melting, Scientific reports, 11, 1-10, 2021.

Alonso-Garcia, M., Sierro, F. J., and Flores, J. A.: Arctic front shifts in the subpolar North Atlantic during the Mid-Pleistocene (800–400 ka) and their implications for ocean circulation, Palaeogeography, Palaeoclimatology, Palaeoecology, 311, 268-280, 2011.

Andrews, J. T.: Icebergs and iceberg rafted detritus (IRD) in the North Atlantic: facts and assumptions, Oceanography, 100-108, 2000.

https://doi.org/10.5194/cp-2023-101
Preprint. Discussion started: 4 January 2024

Arz, H. W., Gerhardt, S., Patzold, J., and Rohl, U.: Millennial-scale changes of surface-and deep-water flow in the western tropical Atlantic linked to Northern Hemisphere high-latitude climate during the Holocene, Geology, 29, 239-242, 2001.

Ashton, N., Lewis, S. G., Parfitt, S. A., Penkman, K. E., and Coope, G. R.: New evidence for complex climate change in MIS 11 from Hoxne, Suffolk, UK, Quaternary Science Reviews, 27, 652-668, 2008.

Bakker, P., Schmittner, A., Lenaerts, J., Abe-Ouchi, A., Bi, D., van den Broeke, M., Chan, W. L., Hu, A., Beadling, R., and Marsland, S.: Fate of the Atlantic Meridional Overturning Circulation: Strong decline under continued warming and Greenland melting, Geophysical Research Letters, 43, 12,252-212,260, 2016.

Balsam, W. L., and McCoy Jr, F. W.: Atlantic sediments: Glacial/interglacial comparisons, Paleoceanography, 2, 531-542, 1987.

Barker, S., Chen, J., Gong, X., Jonkers, L., Knorr, G., and Thornalley, D.: Icebergs not the trigger for North Atlantic cold events, Nature, 520, 333, 2015.

Bauch, H. A., Erlenkeuser, H., Helmke, J. P., and Struck, U.: A paleoclimatic evaluation of marine oxygen isotope stage 11 in the high-northern Atlantic (Nordic seas), Global and Planetary Change, 24, 27-39, http://dx.doi.org/10.1016/S0921-8181(99)00067-3, 2000.

Bazin, L., Landais, A., Lemieux-Dudon, B., Toyé Mahamadou Kele, H., Veres, D., Parrenin, F., Martinerie, P., Ritz, C., Capron, E., and Lipenkov, V.: An optimized multi-proxy, multi-site Antarctic ice and gas orbital chronology (AICC2012): 120–800 ka, Clim Past, 9, 1715-1731, 2013.

Bendle, J., Rosell-Melé, A., and Ziveri, P.: Variability of unusual distributions of alkenones in the surface waters of the Nordic seas, Paleoceanography, 20, 2005.

Berger, A., and Loutre, M. F.: Insolation values for the climate of the last 10 million years, Quaternary Science Reviews, 10, 297-317, 1991.

Berger, A., and Loutre, M.-F.: An exceptionally long interglacial ahead?, Science, 297, 1287-1288, 2002.

Berk, J. v. d., Drijfhout, S., and Hazeleger, W.: Circulation adjustment in the Arctic and Atlantic in response to Greenland and Antarctic mass loss, Climate Dynamics, 57, 1689-1707, 2021.

Bond, G., Showers, W., Cheseby, M., Lotti, R., Almasi, P., DeMenocal, P., Priore, P., Cullen, H., Hajdas, I., and Bonani, G.: A pervasive millennial-scale cycle in North Atlantic Holocene and glacial climates, science, 278, 1257-1266, 1997.

Böning, C. W., Behrens, E., Biastoch, A., Getzlaff, K., and Bamber, J. L.: Emerging impact of Greenland meltwater on deepwater formation in the North Atlantic Ocean, Nature Geoscience, 9, 523-527, 2016.

Born, A., Stocker, T. F., Raible, C. C., and Levermann, A.: Is the Atlantic subpolar gyre bistable in comprehensive coupled climate models?, Climate dynamics, 40, 2993-3007, 2013.

Born, A., and Stocker, T. F.: Two stable equilibria of the Atlantic subpolar gyre, Journal of Physical Oceanography, 44, 246-264, 2014.

https://doi.org/10.5194/cp-2023-101
Preprint. Discussion started: 4 January 2024

Breitenbach, S. F. M., Rehfeld, K., Goswami, B., Baldini, J. U., Ridley, H. E., Kennett, D. J., Prufer, K. M., Aquino, V. V., Asmerom, Y., and Polyak, V. J.: Constructing proxy records from age models (COPRA), Clim Past, 8, 1765-1779, 2012.

Brodeau, L., and Koenigk, T.: Extinction of the northern oceanic deep convection in an ensemble of climate model simulations of the 20th and 21st centuries, Climate Dynamics, 46, 2863-2882, 2016.

Buckley, M. W., and Marshall, J.: Observations, inferences, and mechanisms of the Atlantic Meridional Overturning Circulation: A review, Reviews of Geophysics, 54, 5-63, 2016.

Caesar, L., Rahmstorf, S., Robinson, A., Feulner, G., and Saba, V.: Observed fingerprint of a weakening Atlantic Ocean overturning circulation, Nature, 556, 191-196, 2018.

Caesar, L., McCarthy, G., Thornalley, D., Cahill, N., and Rahmstorf, S.: Current Atlantic Meridional Overturning Circulation weakest in last millennium, Nature Geoscience, 1-3, 2021.

Candy, I., Schreve, D. C., Sherriff, J., and Tye, G. J.: Marine Isotope Stage 11: Palaeoclimates, palaeoenvironments and its role as an analogue for the current interglacial, Earth-Science Reviews, 128, 18-51, http://dx.doi.org/10.1016/j.earscirev.2013.09.006, 2014.

Chapman, M. R.: Seasonal production patterns of planktonic foraminifera in the NE Atlantic Ocean: Implications for paleotemperature and hydrographic reconstructions, Paleoceanography, 25, 2010.

Chen, W., and Guillaume, M.: HALS-based NMF with flexible constraints for hyperspectral unmixing, EURASIP Journal on Advances in Signal Processing, 2012, 54, 2012.

Christ, A. J., Rittenour, T. M., Bierman, P. R., Keisling, B. A., Knutz, P. C., Thomsen, T. B., Keulen, N., Fosdick, J. C., Hemming, S. R., and Tison, J.-L.: Deglaciation of northwestern Greenland during Marine Isotope Stage 11, Science, 381, 330-335, 2023.

Clemens, S. C.: An astronomical tuning strategy for Pliocene sections: implications for global-scale correlation and phase relationships, Philosophical Transactions of the Royal Society of London. Series A: Mathematical, Physical and Engineering Sciences, 357, 1949-1973, 1999.

CLIMAP, and Members, C. P.: The surface of the ice age earth, Science, 191, 1131-1137, 1976.

Crow, B. R., Prange, M., and Schulz, M.: Dynamic boreal summer atmospheric circulation response as negative feedback to Greenland melt during the MIS-11 interglacial, Climate of the Past, 18, 775-792, 2022.

de Vernal, A., and Hillaire-Marcel, C.: Natural Variability of Greenland Climate, Vegetation, and Ice Volume During the Past Million Years, Science, 320, 1622-1625, 10.1126/science.1153929, 2008.

Desprat, S., Goñi, M. F. S., Turon, J.-L., McManus, J. F., Loutre, M. F., Duprat, J., Malaizé, B., Peyron, O., and Peypouquet, J.-P.: Is vegetation responsible for glacial inception during periods of muted insolation changes?, Quaternary Science Reviews, 24, 1361-1374, 2005a.

Desprat, S., Goñi, M. S., Turon, J.-L., McManus, J., Loutre, M.-F., Duprat, J., Malaize, B., Peyron, O., and Peypouquet, J.-P.: Is vegetation responsible for glacial inception during periods of muted insolation changes?, Quaternary Science Reviews, 24, 1361-1374, 2005b.

Dickson, A. J., Beer, C. J., Dempsey, C., Maslin, M. A., Bendle, J. A., McClymont, E. L., and Pancost, R. D.: Oceanic forcing of the Marine Isotope Stage 11 interglacial, Nature Geoscience, 2, 428, 2009.

https://doi.org/10.5194/cp-2023-101
Preprint. Discussion started: 4 January 2024

Dickson, A. J., Leng, M. J., Maslin, M. A., Sloane, H. J., Green, J., Bendle, J. A., McClymont, E. L., and Pancost, R. D.: Atlantic overturning circulation and Agulhas leakage influences on southeast Atlantic upper ocean hydrography during marine isotope stage 11, Paleoceanography, 25, 2010.

Doherty, J. M., and Thibodeau, B.: Cold water in a warm world: Investigating the origin of the Nordic seas' unique surface properties during MIS 11, Frontiers in Marine Science, 5, 251, 2018.

Doherty, J. M., Ling, Y. F., Not, C., Erler, D., Bauch, H. A., Paytan, A., and Thibodeau, B.: Freshening, stratification and deep-water formation in the Nordic Seas during marine isotope stage 11, Quaternary Science Reviews, 272, 107231, 2021.

Drijfhout, S.: Competition between global warming and an abrupt collapse of the AMOC in Earth’s energy imbalance, Scientific reports, 5, 14877, 2015.

Droxler, A. W., Poore, R. Z., and Burckle, L. H.: Earth's Climate and Orbital Eccentricity: The Marine Isotope Stage 11 Question, Geophys. Monogr. Ser., edited by: Droxler, A. W., Poore, R. Z., and Burckle, L. H., AGU, Washington, DC, 240 pp., 2003.

Dubois-Dauphin, Q., Colin, C., Bonneau, L., Montagna, P., Wu, Q., Van Rooij, D., Reverdin, G., Douville, E., Thil, F., and Waldner, A.: Fingerprinting Northeast Atlantic water masses using neodymium isotopes, Geochimica et Cosmochimica Acta, 210, 267-288, 2017.

Eide, M., Olsen, A., Ninnemann, U. S., and Johannessen, T.: A global ocean climatology of preindustrial and modern ocean δ13C, Global Biogeochemical Cycles, 31, 515-534, doi:10.1002/2016GB005473, 2017.

Eldevik, T., Risebrobakken, B., Bjune, A. E., Andersson, C., Birks, H. J. B., Dokken, T. M., Drange, H., Glessmer, M. S., Li, C., and Nilsen, J. E. Ø.: A brief history of climate–the northern seas from the Last Glacial Maximum to global warming, Quaternary Science Reviews, 106, 225-246, 2014.

Ellett, D., and Martin, J.: The physical and chemical oceanography of the Rockall Channel, Deep Sea Research and Oceanographic Abstracts, 1973, 585-625,

Ellett, D., Edwards, A., and Bowers, R.: The hydrography of the Rockall Channel—an overview, Proceedings of the Royal Society of Edinburgh, Section B: Biological Sciences, 88, 61-81, 1986.

Fettweis, X., Box, J. E., Agosta, C., Amory, C., Kittel, C., Lang, C., van As, D., Machguth, H., and Gallée, H.: Reconstructions of the 1900–2015 Greenland ice sheet surface mass balance using the regional climate MAR model, The Cryosphere, 11, 1015-1033, 2017.

Flood, R. D., Hollister, C., and Lonsdale, P.: Disruption of the Feni sediment drift by debris flows from Rockall Bank, Marine Geology, 32, 311-334, 1979.

Fraile, I., Mulitza, S., and Schulz, M.: Modeling planktonic foraminiferal seasonality: Implications for sea-surface temperature reconstructions, Marine Micropaleontology, 72, 1-9, 10.1016/j.marmicro.2009.01.003, 2009.

Galaasen, E. V., Ninnemann, U. S., Irvalı, N., Kleiven, H. F., Rosenthal, Y., Kissel, C., and Hodell, D. A.: Rapid Reductions in North Atlantic Deep Water During the Peak of the Last Interglacial Period, Science, 343, 1129-1132, 10.1126/science.1248667, 2014.

https://doi.org/10.5194/cp-2023-101
Preprint. Discussion started: 4 January 2024

Galaasen, E. V., Ninnemann, U. S., Kessler, A., Irvalı, N., Rosenthal, Y., Tjiputra, J., Bouttes, N., Roche, D. M., Kleiven, H. K. F., and Hodell, D. A.: Interglacial instability of North Atlantic deep water ventilation, Science, 367, 1485-1489, 2020.

Gebhardt, H., Sarnthein, M., Grootes, P. M., Kiefer, T., Kuehn, H., Schmieder, F., and Röhl, U.: Paleonutrient and productivity records from the subarctic North Pacific for Pleistocene glacial terminations I to V, Paleoceanography, 23, 2008.

Golledge, N. R., Keller, E. D., Gomez, N., Naughten, K. A., Bernales, J., Trusel, L. D., and Edwards, T. L.: Global environmental consequences of twenty-first-century ice-sheet melt, Nature, 566, 65-72, 2019.

Hansen, B., and Østerhus, S.: North Atlantic Nordic Seas exchanges, Progress in Oceanography, 45, 109-208, 2000.

Hátún, H., Sandø, A. B., Drange, H., Hansen, B., and Valdimarsson, H.: Influence of the Atlantic subpolar gyre on the thermohaline circulation, Science, 309, 1841-1844, 2005.

Haug, G. H., Hughen, K. A., Sigman, D. M., Peterson, L. C., and Röhl, U.: Southward migration of the intertropical convergence zone through the Holocene, Science, 293, 1304-1308, 2001.

Helmke, J. P., and Bauch, H. A.: Comparison of glacial and interglacial conditions between the polar and subpolar North Atlantic region over the last five climatic cycles, Paleoceanography, 18, 2003.

Hodell, D. A., Charles, C. D., and Ninnemann, U. S.: Comparison of interglacial stages in the South Atlantic sector of the southern ocean for the past 450 kyr: implifications for Marine Isotope Stage (MIS) 11, Global and Planetary Change, 24, 7-26, 2000.

Hodell, D. A., Channell, J. E., Curtis, J. H., Romero, O. E., and Röhl, U.: Onset of “Hudson Strait” Heinrich events in the eastern North Atlantic at the end of the middle Pleistocene transition (∼ 640 ka)?, Paleoceanography, 23, 2008.

Holliday, N. P., Pollard, R. T., Read, J. F., and Leach, H.: Water mass properties and fluxes in the Rockall Trough, 1975-1998, Deep Sea Research Part I, 47, 1303-1332, 2000.

Holmes, D. E., Babila, T. L., Ninnemann, U., Bromley, G., Tyrrell, S., Paterson, G. A., Curran, M. J., and Morley, A.: Reorganization of Atlantic Waters at sub-polar latitudes linked to deep-water overflow in both glacial and interglacial climate states, Climate of the Past, 18, 989-1009, 2022.

Howard, W. R.: Palaeoclimatology: A warm future in the past, Nature, 388, 418, 1997.

Hutson, W. H.: The Agulhas Current during the late Pleistocene: Analysis of modern faunal analogs, Science, 207, 64-66, 1980.

Imbrie, J., and Kipp, N. G.: A new micropaleontological method for quantitative paleoclimatology: application to a late Pleistocene Caribbean core, in: The Late Cenozoic Glacial Ages, edited by: Turekian, K. K., Yale Univ. Press, New Haven, 71-181, 1971.

Irvalı, N., Ninnemann, U. S., Kleiven, H. K. F., Galaasen, E. V., Morley, A., and Rosenthal, Y.: Evidence for regional cooling, frontal advances, and East Greenland Ice Sheet changes during the demise of the last interglacial, Quaternary Science Reviews, 150, 184-199, 2016.

Irvalı, N., Galaasen, E. V., Ninnemann, U. S., Rosenthal, Y., Born, A., and Kleiven, H. K. F.: A low climate threshold for south Greenland Ice Sheet demise during the Late Pleistocene, Proceedings of the National Academy of Sciences, 117, 190-195, 2020.

Jacobsen, S. B., and Wasserburg, G.: Sm-Nd isotopic evolution of chondrites, Earth and Planetary Science Letters, 50, 139-155, 1980.

Johannessen, T., Jansen, E., Flatøy, A., and Ravelo, A. C.: The relationship between surface water masses, oceanographic fronts and paleoclimatic proxies in surface sediments of the Greenland, Iceland, Norwegian Seas, in: Carbon cycling in the glacial ocean: constraints on the ocean's role in global change, Springer, 61-85, 1994.

Johnson, C., Sherwin, T., Smythe-Wright, D., Shimmield, T., and Turrell, W.: Wyville Thomson Ridge overflow water: spatial and temporal distribution in the Rockall Trough, Deep Sea Research Part I: Oceanographic Research Papers, 57, 1153-1162, 2010.

Johnson, C., Sherwin, T., Cunningham, S., Dumont, E., Houpert, L., and Holliday, N. P.: Transports and pathways of overflow water in the Rockall Trough, Deep Sea Research Part I: Oceanographic Research Papers, 122, 48-59, 2017.

Jonkers, L., Prins, M. A., Moros, M., Weltje, G. J., Troelstra, S. R., and Brummer, G.-J. A.: Temporal offsets between surface temperature, ice-rafting and bottom flow speed proxies in the glacial (MIS 3) northern North Atlantic, Quaternary Science Reviews, 48, 43-53, 2012.

Jonkers, L., Van Heuven, S., Zahn, R., and Peeters, F. J.: Seasonal patterns of shell flux, δ18O and δ13C of small and large N. pachyderma (s) and G. bulloides in the subpolar North Atlantic, Paleoceanography, 28, 164-174, 2013.

Jonkers, L., Barker, S., Hall, I. R., and Prins, M. A.: Correcting for the influence of ice-rafted detritus on grain size-based paleocurrent speed estimates, Paleoceanography, 30, 1347-1357, 2015.

Juggins, S.: Rioja: analysis of Quaternary Science Data: R package versión (0.9–21). 2017.

Jungclaus, J., Haak, H., Esch, M., Roeckner, E., and Marotzke, J.: Will Greenland melting halt the thermohaline circulation?, Geophysical Research Letters, 33, 2006a.

Jungclaus, J. H., Haak, H., Esch, M., Roeckner, E., and Marotzke, J.: Will Greenland melting halt the thermohaline circulation?, Geophys. Res. Lett., 33, 10.1029/2006gl026815, 2006b.

Kandiano, E. S., and Bauch, H. A.: Phase relationship and surface water mass change in the Northeast Atlantic during Marine Isotope Stage 11 (MIS 11), Quaternary Research, 68, 445-455, http://dx.doi.org/10.1016/j.yqres.2007.07.009, 2007.

Kandiano, E. S., Bauch, H. A., Fahl, K., Helmke, J. P., Röhl, U., Pérez-Folgado, M., and Cacho, I.: The meridional temperature gradient in the eastern North Atlantic during MIS 11 and its link to the ocean–atmosphere system, Palaeogeography, Palaeoclimatology, Palaeoecology, 333, 24-39, 2012.

Kandiano, E. S., Meer, M. T., Bauch, H. A., Helmke, J., Damsté, J. S. S., and Schouten, S.: A cold and fresh ocean surface in the Nordic Seas during MIS 11: Significance for the future ocean, Geophysical Research Letters, 43, 2016.

https://doi.org/10.5194/cp-2023-101
Preprint. Discussion started: 4 January 2024

Climate of the Past
Discussions

Kandiano, E. S., Van der Meer, M. T., Schouten, S., Fahl, K., Damsté, J. S. S., and Bauch, H. A.: Response of the North Atlantic surface and intermediate ocean structure to climate warming of MIS 11, Scientific reports, 7, 1-9, 2017a.

Kandiano, E. S., Van Der Meer, M. T., Schouten, S., Fahl, K., Damsté, J. S. S., and Bauch, H. A.: Response of the North Atlantic surface and intermediate ocean structure to climate warming of MIS 11, Scientific Reports, 7, 2017b.

Kessler, A., Bouttes, N., Roche, D. M., Ninnemann, U. S., and Tjiputra, J.: Dynamics of spontaneous (multi) centennial-scale variations of the Atlantic meridional overturning circulation strength during the last interglacial, Paleoceanography and Paleoclimatology, 35, e2020PA003913, 2020.

Kipp, N. G.: New transfer function for estimating past sea-surface conditions from sea-bed distribution of planktonic foraminiferal assemblages in the North Atlantic, Geol. Soc. Amer. Mem., 145, 3-41, 1976.

Kohfeld, K. E., Fairbanks, R. G., Smith, S. L., and Walsh, I. D.: Neogloboquadrina pachyderma (sinistral coiling) as paleoceanographic tracers in polar oceans: Evidence from Northeast Water Polynya plankton tows, sediment traps, and surface sediments, Paleoceanography, 11, 679-699, 1996.

Kretschmer, K., Jonkers, L., Kucera, M., and Schulz, M.: Modeling seasonal and vertical habitats of planktonic foraminifera on a global scale, Biogeosciences, 15, 4405-4429, 2018.

Lambelet, M., Van De Flierdt, T., Crocket, K., Rehkämper, M., Kreissig, K., Coles, B., Rijkenberg, M. J., Gerringa, L. J., de Baar, H. J., and Steinfeldt, R.: Neodymium isotopic composition and concentration in the western North Atlantic Ocean: Results from the GEOTRACES GA02 section, Geochimica et Cosmochimica Acta, 177, 1-29, 2016.

Laskar, J., Robutel, P., Joutel, F., Gastineau, M., Correia, A. C. M., and Levrard, B.: A long-term numerical solution for the insolation quantities of the Earth, A&A, 428, 261-285, 2004.

Latif, M., Böning, C., Willebrand, J., Biastoch, A., Dengg, J., Keenlyside, N., Schweckendiek, U., and Madec, G.: Is the thermohaline circulation changing?, Journal of Climate, 19, 4631-4637, 2006.

Le Bras, I. A. A., Straneo, F., Holte, J., and Holliday, N. P.: Seasonality of freshwater in the East Greenland Current system from 2014 to 2016, Journal of Geophysical Research: Oceans, 123, 8828-8848, 2018.

Lisiecki, L. E., and Raymo, M. E.: A Pliocene-Pleistocene stack of 57 globally distributed benthic δ18O records, Paleoceanography, 20, 2005.

Lofverstrom, M., Thompson, D. M., Otto-Bliesner, B. L., and Brady, E. C.: The importance of Canadian Arctic Archipelago gateways for glacial expansion in Scandinavia, Nature Geoscience, 15, 482-488, 2022.

Lohmann, J., and Ditlevsen, P. D.: Risk of tipping the overturning circulation due to increasing rates of ice melt, Proceedings of the National Academy of Sciences, 118, e2017989118, 2021.

Loubere, P.: Oceanographic parameters reflected in the seabed distribution of planktic foraminifera from the North Atlantic and Mediterranean Sea, The Journal of Foraminiferal Research, 11, 137-158, 1981.

Loutre, M.-F., and Berger, A.: Future climatic changes: Are we entering an exceptionally long interglacial?, Climatic Change, 46, 61-90, 2000.

Loutre, M.-F., and Berger, A.: Marine Isotope Stage 11 as an analogue for the present interglacial, Global and planetary change, 36, 209-217, 2003.

Luo, H., Castelao, R. M., Rennermalm, A. K., Tedesco, M., Bracco, A., Yager, P. L., and Mote, T. L.: Oceanic transport of surface meltwater from the southern Greenland ice sheet, Nature Geoscience, 9, 528-532, 2016.

Mauritzen, C.: Production of dense overflow waters feeding the North Atlantic across the Greenland-Scotland Ridge. Part 1: Evidence for a revised circulation scheme, Deep Sea Research Part I: Oceanographic Research Papers, 43, 769-806, 1996.

Mcmanus, J., Oppo, D., Cullen, J., and Healey, S.: Marine isotope stage 11 (MIS 11): analog for Holocene and future Climate?, Earth's climate and orbital eccentricity: the marine isotope stage 11 question, 69-85, 2003.

McManus, J. F., Oppo, D. W., and Cullen, J. L.: A 0.5-million-year record of millenial scale climate variability in the North Atlantic, Science, 283, 971-975, 1999.

Melles, M., Brigham-Grette, J., Minyuk, P. S., Nowaczyk, N. R., Wennrich, V., DeConto, R. M., Anderson, P. M., Andreev, A. A., Coletti, A., and Cook, T. L.: 2.8 million years of Arctic climate change from Lake El'gygytgyn, NE Russia, science, 337, 315-320, 2012.

Mokeddem, Z., McManus, J. F., and Oppo, D. W.: Oceanographic dynamics and the end of the last interglacial in the subpolar North Atlantic, Proceedings of the National Academy of Sciences, 111, 11263-11268, 10.1073/pnas.1322103111, 2014.

Mudelsee, M.: Ramp function regression: a tool for quantifying climate transitions, Computers & Geosciences, 26, 293-307, 2000.

Müller, W. A., Matei, D., Bersch, M., Jungclaus, J. H., Haak, H., Lohmann, K., Compo, G., Sardeshmukh, P., and Marotzke, J.: A twentieth-century reanalysis forced ocean model to reconstruct the North Atlantic climate variation during the 1920s, Climate Dynamics, 44, 1935-1955, 2015.

Muschitiello, F., D'Andrea, W. J., Schmittner, A., Heaton, T. J., Balascio, N. L., DeRoberts, N., Caffee, M. W., Woodruff, T. E., Welten, K. C., and Skinner, L. C.: Deep-water circulation changes lead North Atlantic climate during deglaciation, Nature communications, 10, 1272, 2019.

Naylor, D., and Shannon, P.: The structural framework of the Irish Atlantic Margin, Geological Society, London, Petroleum Geology Conference Series, 2005, 1009-1021,

Nehrbass-Ahles, C., Shin, J., Schmitt, J., Bereiter, B., Joos, F., Schilt, A., Schmidely, L., Silva, L., Teste, G., and Grilli, R.: Abrupt CO2 release to the atmosphere under glacial and early interglacial climate conditions, Science, 369, 1000-1005, 2020.

Nitychoruk, J., Bińka, K., Hoefs, J., Ruppert, H., and Schneider, J.: Climate reconstruction for the Holsteinian Interglacial in eastern Poland and its comparison with isotopic data from Marine Isotope Stage 11, Quaternary Science Reviews, 24, 631-644, 2005.

https://doi.org/10.5194/cp-2023-101
Preprint. Discussion started: 4 January 2024

Climate of the Past Discussions

Nürnberg, D., Wollenburg, I., Dethleff, D., Eicken, H., Kassens, H., Letzig, T., Reimnitz, E., and Thiede, J.: Sediments in Arctic sea ice: Implications for entrainment, transport and release, Marine geology, 119, 185-214, 1994.

Olsen, S. M., Hansen, B., Quadfasel, D., and Østerhus, S.: Observed and modelled stability of overflow across the Greenland–Scotland ridge, Nature, 455, 519-522, 2008.

Oppo, D. W., McManus, J. F., and Cullen, J. L.: Abrupt climate events 500,000 to 340,000 years ago: evidence from subpolar North Atlantic sediments, Science, 279, 1335-1338, 1998.

Østerhus, S., Turrell, W. R., Hansen, B., Lundberg, P., and Buch, E.: Observed transport estimates between the North Atlantic and the Arctic Mediterranean in the Iceland–Scotland region, Polar research, 20, 169-175, 2001.

PAGES, P. I. W. G. o.: Interglacials of the last 800,000 years, Reviews of Geophysics, 54, 162-219, 2016.

Parker, R. L., Foster, G. L., Gutjahr, M., Wilson, P. A., Obrochta, S. P., Fagel, N., Cooper, M. J., Michalik, A., Milton, J. A., and Bailey, I.: The history of ice-sheet retreat on North America during Termination 5: Implications for the origin of the sea-level highstand during interglacial stage 11, Earth and Planetary Science Letters, 618, 118286, 2023.

Paterson, G. A., and Heslop, D.: New methods for unmixing sediment grain size data, Geochemistry, Geophysics, Geosystems, 16, 4494-4506, 2015.

Petit, J. R., Jouzel, J., Raynaud, D., Barkov, N. I., Barnola, J.-M., Basile, I., Bender, M., Chappellaz, J., Davis, M., Delaygue, G., Delmotte, M., Kotlyakov, V. M., Legrand, M., Lipenkov, V. Y., Lorius, C., Pépin, L., Ritz, C., Saltzman, E., and Stievenard, M.: Climate and atmospheric history of the past 420,000 years from the Vostok ice core, Antarctica, Nature, 399, 429-436, 1999.

Pflaumann, U., Duprat, J., Pujol, C., and Labeyrie, L. D.: SIMMAX: A modern analog technique to deduce Atlantic sea surface temperatures from planktonic foraminifera in deep-sea sediments, Paleoceanography, 11, 15-35, 1996.

Piva, A., Asioli, A., Schneider, R. R., Trincardi, F., Andersen, N., Colmenero-Hidalgo, E., Dennielou, B., Flores, J. A., and Vigliotti, L.: Climatic cycles as expressed in sediments of the PROMESS1 borehole PRAD1-2, central Adriatic, for the last 370 ka: 1. Integrated stratigraphy, Geochemistry, Geophysics, Geosystems, 9, 2008.

Pol, K., Debret, M., Masson-Delmotte, V., Capron, E., Cattani, O., Dreyfus, G., Falourd, S., Johnsen, S., Jouzel, J., and Landais, A.: Links between MIS 11 millennial to sub-millennial climate variability and long term trends as revealed by new high resolution EPICA Dome C deuterium data–A comparison with the Holocene, Clim Past, 7, 437-450, 2011.

Polakowski, C., Ryżak, M., Sochan, A., Beczek, M., Mazur, R., and Bieganowski, A.: Particle Size Distribution of Various Soil Materials Measured by Laser Diffraction—The Problem of Reproducibility, Minerals, 11, 465, 2021.

Praetorius, S. K., McManus, J. F., Oppo, D. W., and Curry, W. B.: Episodic reductions in bottom-water currents since the last ice age, Nature Geoscience, 1, 449-452, 2008.

https://doi.org/10.5194/cp-2023-101
Preprint. Discussion started: 4 January 2024

Preece, R., Parfitt, S., Bridgland, D., Lewis, S., Rowe, P., Atkinson, T., Candy, I., Debenham, N., Penkman, K., and Rhodes, E.: Terrestrial environments during MIS 11: evidence from the Palaeolithic site at West Stow, Suffolk, UK, Quaternary Science Reviews, 26, 1236-1300, 2007.

Prell, W. L.: Stability of low-latitude sea-surface temperatures: an evaluation of the CLIMAP reconstruction with emphasis on the positive SST anomalies. Final report, Brown Univ., Providence, RI (USA). Dept. of Geological Sciences, 1985.

Prins, M. A., Bouwer, L. M., Beets, C. J., Troelstra, S. R., Weltje, G. J., Kruk, R. W., Kuijpers, A., and Vroon, P. Z.: Ocean circulation and iceberg discharge in the glacial North Atlantic: Inferences from unmixing of sediment size distributions, Geology, 30, 555-558, 2002.

Prokopenko, A., Bezrukova, E., Khursevich, G., Solotchina, E., Kuzmin, M., and Tarasov, P.: Climate in continental interior Asia during the longest interglacial of the past 500 000 years: the new MIS 11 records from Lake Baikal, SE Siberia, Climate of the Past, 6, 31-48, 2010.

Rachmayani, R., Prange, M., Lunt, D. J., Stone, E. J., and Schulz, M.: Sensitivity of the Greenland Ice Sheet to Interglacial Climate Forcing: MIS 5e Versus MIS 11, Paleoceanography, 32, 1089-1101, doi:10.1002/2017PA003149, 2017.

Rahmstorf, S.: Bifurcations of the Atlantic thermohaline circulation in response to changes in the hydrological cycle, Nature, 378, 145-149, 1995.

Raymo, M. E., and Mitrovica, J. X.: Collapse of polar ice sheets during the stage 11 interglacial, Nature, 483, 453-456, 2012.

Raynaud, D., Barnola, J.-M., Souchez, R., Lorrain, R., Petit, J.-R., Duval, P., and Lipenkov, V. Y.: The record for marine isotopic stage 11, Nature, 436, 39-40, 2005.

Rebolledo, L., Sepúlveda, J., Lange, C. B., Pantoja, S., Bertrand, S., Hughen, K., and Figueroa, D.: Late Holocene marine productivity changes in Northern Patagonia-Chile inferred from a multi-proxy analysis of Jacaf channel sediments, Estuarine, Coastal and Shelf Science, 80, 314-322, 2008.

Reille, M., Beaulieu, J. L. D., Svobodova, H., Andrieu-Ponel, V., and Goeury, C.: Pollen analytical biostratigraphy of the last five climatic cycles from a long continental sequence from the Velay region (Massif Central, France), Journal of Quaternary Science: Published for the Quaternary Research Association, 15, 665-685, 2000.

Reyes, A. V., Carlson, A. E., Beard, B. L., Hatfield, R. G., Stoner, J. S., Winsor, K., Welke, B., and Ullman, D. J.: South Greenland ice-sheet collapse during marine isotope stage 11, Nature, 510, 525, 2014.

Risebrobakken, B., Dokken, T., Smedsrud, L. H., Andersson, C., Jansen, E., Moros, M., and Ivanova, E. V.: Early Holocene temperature variability in the Nordic Seas: The role of oceanic heat advection versus changes in orbital forcing, Paleoceanography, 26, 2011.

Riveiros, N. V., Waelbroeck, C., Skinner, L., Duplessy, J.-C., McManus, J. F., Kandiano, E. S., and Bauch, H. A.: The "MIS 11 paradox" and ocean circulation: Role of millennial scale events, Earth and Planetary Science Letters, 371, 258-268, 2013.

Robinson, A., Calov, R., and Ganopolski, A.: Multistability and critical thresholds of the Greenland ice sheet, Nature Climate Change, 2, 429-432, 2012.

https://doi.org/10.5194/cp-2023-101
Preprint. Discussion started: 4 January 2024

Robinson, A., Alvarez-Solas, J., Calov, R., Ganopolski, A., and Montoya, M.: MIS-11 duration key to disappearance of the Greenland ice sheet, Nature communications, 8, 16008, 2017a.

Robinson, A., Alvarez-Solas, J., Calov, R., Ganopolski, A., and Montoya, M.: MIS-11 duration key to disappearance of the Greenland ice sheet, Nature communications, 8, 1-7, 2017b.

Robinson, S. G., and McCave, I. N.: Orbital forcing of bottom-current enhanced sedimentation on Feni Drift, NE Atlantic, during the mid-Pleistocene, Paleoceanography, 9, 943-972, 1994.

Rothwell, R. G.: Micro-XRF studies of sediment cores: a perspective on capability and application in the environmental sciences, in: Micro-XRF studies of sediment cores, Springer, 1-21, 2015.

Ruddiman, W. F.: Late Quaternary deposition of ice-rafted sand in the subpolar North Atlantic (lat 40° to 65°N), Geol. Soc. Am. Bull., 88, 1813-1827, 1977.

Ruddiman, W. F.: Cold climate during the closest stage 11 analog to recent millennia, Quaternary Science Reviews, 24, 1111-1121, 2005.

Sandø, A. B., Nilsen, J. E. Ø., Eldevik, T., and Bentsen, M.: Mechanisms for variable North Atlantic–Nordic seas exchanges, Journal of Geophysical Research: Oceans, 117, https://doi.org/10.1029/2012JC008177, 2012.

Sgubin, G., Swingedouw, D., Drijfhout, S., Mary, Y., and Bennabi, A.: Abrupt cooling over the North Atlantic in modern climate models, Nature Communications, 8, 1-12, 2017a.

Sgubin, G., Swingedouw, D., Drijfhout, S., Mary, Y., and Bennabi, A.: Abrupt cooling over the North Atlantic in modern climate models, Nature Communications, 8, 2017b.

SHICHI, K., TAKAHARA, H., and KAWAMURO, K.: Vegetation and climate changes during MIS 11 in southeastern Siberia based on pollen records from Lake Baikal sediment, Japanese Journal of Palynology, 55, 3-14, 2009.

Siccha, M., and Kucera, M.: ForCenS, a curated database of planktonic foraminifera census counts in marine surface sediment samples, Scientific data, 4, 170109, 2017.

Smeed, D. A., McCarthy, G. D., Cunningham, S. A., Frajka-Williams, E., Rayner, D., Johns, W. E., Meinen, C. S., Baringer, M. O., Moat, B. I., and Duchez, A.: Observed decline of the Atlantic meridional overturning circulation 2004–2012, Ocean Science, 10, 29-38, 2014.

Smeed, D. A., Josey, S., Beaulieu, C., Johns, W. E., Moat, B. I., Frajka-Williams, E., Rayner, D., Meinen, C. S., Baringer, M. O., and Bryden, H. L.: The North Atlantic Ocean is in a state of reduced overturning, Geophysical Research Letters, 45, 1527-1533, 2018.

Solignac, S., Seidenkrantz, M.-S., Jessen, C., Kuijpers, A., Gunvald, A. K., and Olsen, J.: Late-Holocene sea-surface conditions offshore Newfoundland based on dinoflagellate cysts, The Holocene, 21, 539-552, 2011.

Stommel, H.: Thermohaline convection with two stable regimes of flow, Tellus, 13, 224-230, 1961.

Stouffer, R. J., Yin, J., Gregory, J., Dixon, K., Spelman, M., Hurlin, W., Weaver, A., Eby, M., Flato, G., and Hasumi, H.: Investigating the causes of the response of the thermohaline circulation to past and future climate changes, Journal of Climate, 19, 1365-1387, 2006.

https://doi.org/10.5194/cp-2023-101
Preprint. Discussion started: 4 January 2024

Sutton, R., and Allen, M. R.: Decadal predictability of North Atlantic sea surface temperature and climate, Nature, 388, 563-567, 1997.

Swingedouw, D., Rodehacke, C. B., Behrens, E., Menary, M., Olsen, S. M., Gao, Y., Mikolajewicz, U., Mignot, J., and Biastoch, A.: Decadal fingerprints of freshwater discharge around Greenland in a multi-model ensemble, Climate Dynamics, 41, 695-720, 2013.

Tanaka, T., Togashi, S., Kamioka, H., Amakawa, H., Kagami, H., Hamamoto, T., Yuhara, M., Orihashi, Y., Yoneda, S., and Shimizu, H.: JNdi-1: a neodymium isotopic reference in consistency with LaJolla neodymium, Chemical Geology, 168, 279-281, 2000.

Team, R. C.: R: A Language and Environment for Statistical Computing (Version 3.5. 2, R Foundation for Statistical Computing, Vienna, Austria, 2018), There is no corresponding record for this reference.[Google Scholar], 2019.

Tedesco, M., and Fettweis, X.: 21st century projections of surface mass balance changes for major drainage systems of the Greenland ice sheet, Environmental Research Letters, 7, 045405, 2012.

Telesiński, M. M., Łącka, M., Kujawa, A., and Zajączkowski, M.: The significance of Atlantic Water routing in the Nordic Seas: the Holocene perspective, The Holocene, 32, 1104-1116, 2022.

Telford, R. J., Heegaard, E., and Birks, H. J. B.: All age–depth models are wrong: but how badly?, Quaternary science reviews, 23, 1-5, 2004.

Thibodeau, B., Bauch, H. A., and Pedersen, T. F.: Stratification-induced variations in nutrient utilization in the Polar North Atlantic during past interglacials, Earth and Planetary Science Letters, 457, 127-135, 2017.

Thornalley, D. J., Oppo, D. W., Ortega, P., Robson, J. I., Brierley, C. M., Davis, R., Hall, I. R., Moffa-Sanchez, P., Rose, N. L., and Spooner, P. T.: Anomalously weak Labrador Sea convection and Atlantic overturning during the past 150 years, Nature, 556, 227, 2018.

Tibshirani, R. J., and Efron, B.: An introduction to the bootstrap, Monographs on statistics and applied probability, 57, 1-436, 1993.

Trachsel, M., and Telford, R. J.: All age–depth models are wrong, but are getting better, The Holocene, 27, 860-869, 2017.

Tzedakis, P., Andrieu, V., De Beaulieu, J.-L., Crowhurst, S. d., Follieri, M., Hooghiemstra, H., Magri, D., Reille, M., Sadori, L., and Shackleton, N.: Comparison of terrestrial and marine records of changing climate of the last 500,000 years, Earth and Planetary Science Letters, 150, 171-176, 1997.

Tzedakis, P., Hooghiemstra, H., and Pälike, H.: The last 1.35 million years at Tenaghi Philippon: revised chronostratigraphy and long-term vegetation trends, Quaternary Science Reviews, 25, 3416-3430, 2006.

Tzedakis, P.: The MIS 11–MIS 1 analogy, southern European vegetation, atmospheric methane and the" early anthropogenic hypothesis", Clim Past, 6, 131-144, 2010.

Tzedakis, P., Wolff, E., Skinner, L., Brovkin, V., Hodell, D., McManus, J. F., and Raynaud, D.: Can we predict the duration of an interglacial?, 2012.

https://doi.org/10.5194/cp-2023-101
Preprint. Discussion started: 4 January 2024

Van Rooij, D., Blamart, D., Richter, T., Wheeler, A., Kozachenko, M., and Henriet, J.-P.: Quaternary sediment dynamics in the Belgica mound province, Porcupine Seabight: ice-rafting events and contour current processes, International Journal of Earth Sciences, 96, 121, 2007.

Vellinga, M., Dickson, B., and Curry, R.: The changing view on how freshwater impacts the Atlantic Meridional Overturning Circulation, in: Arctic–subarctic ocean fluxes: Defining the role of the northern seas in climate, Springer, 289-313, 2008.

Waelbroeck, C., Labeyrie, L., Duplessy, J. C., Guiot, J., Labracherie, M., Leclaire, H., and Duprat, J.: Improving past sea surface temperature estimates based on planktonic fossil faunas, Paleoceanography, 13, 272-283, 1998.

Weltje, G. J.: End-member modeling of compositional data: Numerical-statistical algorithms for solving the explicit mixing problem, Mathematical Geology, 29, 503-549, 1997.

Wood, R. A., Keen, A. B., Mitchell, F. B., and Gregory, J. M.: Changing spatial structure of the thermohaline circulation on response to atmospheric CO2 forcing in a climate model, Nature, 399, 572-575, 1999.

Worthington, E. L., Moat, B. I., Smeed, D. A., Mecking, J. V., Marsh, R., and McCarthy, G. D.: A 30-year reconstruction of the Atlantic meridional overturning circulation shows no decline, Ocean Sci., 17, 285-299, 10.5194/os-17-285-2021, 2021.

Wu, Q., Colin, C., Liu, Z., Douville, E., Dubois-Dauphin, Q., and Frank, N.: New insights into hydrological exchange between the South China Sea and the Western Pacific Ocean based on the Nd isotopic composition of seawater, Deep Sea Research Part II: Topical Studies in Oceanography, 122, 25-40, 2015.

Yin, Q., and Berger, A.: Interglacial analogues of the Holocene and its natural near future, Quaternary Science Reviews, 120, 28-46, 2015.

Yu, L., Gao, Y., and Otterå, O. H.: The sensitivity of the Atlantic meridional overturning circulation to enhanced freshwater discharge along the entire, eastern and western coast of Greenland, Climate Dynamics, 46, 1351-1369, 2016.